



RESEARCH ARTICLE

10.1002/2016JD025756

Key Points:

- Monthly mean surface [Cl] $>10^4$ atoms cm^{-3} in polluted northern hemisphere
- Cl atoms account for up to 25% of regional boundary layer CH_4 oxidation
- Global tropospheric sink of $\sim 12\text{--}13$ Tg CH_4/yr from $\text{CH}_4 + \text{Cl}$ reaction ($\sim 2.5\%$ of total CH_4 oxidation)

Supporting Information:

- Supporting Information S1

Correspondence to:

R. Hossaini,
r.hossaini@lancaster.ac.uk

Citation:

Hossaini, R., M. P. Chipperfield, A. Saiz-Lopez, R. Fernandez, S. Monks, W. Feng, P. Brauer, and R. von Glasow (2016), A global model of tropospheric chlorine chemistry: Organic versus inorganic sources and impact on methane oxidation, *J. Geophys. Res. Atmos.*, 121, 14,271–14,297, doi:10.1002/2016JD025756.

Received 8 AUG 2016

Accepted 13 NOV 2016

Accepted article online 16 NOV 2016

Published online 15 DEC 2016

A global model of tropospheric chlorine chemistry: Organic versus inorganic sources and impact on methane oxidation

Ryan Hossaini¹ , Martyn P. Chipperfield² , Alfonso Saiz-Lopez³, Rafael Fernandez^{3,4} , Sarah Monks^{5,6} , Wuhu Feng², Peter Brauer^{7,8} , and Roland von Glasow⁷

¹Lancaster Environment Centre, University of Lancaster, Lancaster, UK, ²School of Earth and Environment, University of Leeds, Leeds, UK, ³Department of Atmospheric Chemistry and Climate, Institute of Physical Chemistry Rocasolano, CSIC, Madrid, Spain, ⁴National Research Council (CONICET), FCEN-UNCuyo, UTN-FRM, Mendoza, Argentina, ⁵Chemical Sciences Division, Earth System Research Laboratory, National Oceanic and Atmospheric Administration, Boulder, Colorado, USA, ⁶Cooperative Institute for Research in Environmental Sciences, University of Colorado Boulder, Boulder, Colorado, USA, ⁷School of Environmental Sciences, University of East Anglia, Norwich, UK, ⁸Wolfson Atmospheric Chemistry Laboratories, Department of Chemistry, University of York, York, UK

Abstract Chlorine atoms (Cl) are highly reactive toward hydrocarbons in the Earth's troposphere, including the greenhouse gas methane (CH_4). However, the regional and global CH_4 sink from Cl is poorly quantified as tropospheric Cl concentrations ([Cl]) are uncertain by ~ 2 orders of magnitude. Here we describe the addition of a detailed tropospheric chlorine scheme to the TOMCAT chemical transport model. The model includes several sources of tropospheric inorganic chlorine (Cl_y), including (i) the oxidation of chlorocarbons of natural (CH_3Cl , CHBr_2Cl , CH_2BrCl , and CHBrCl_2) and anthropogenic (CH_2Cl_2 , CHCl_3 , C_2Cl_4 , C_2HCl_3 , and $\text{CH}_2\text{ClCH}_2\text{Cl}$) origin and (ii) sea-salt aerosol dechlorination. Simulations were performed to quantify tropospheric [Cl], with a focus on the marine boundary layer, and quantify the global significance of Cl atom CH_4 oxidation. In agreement with observations, simulated surface levels of hydrogen chloride (HCl), the most abundant Cl_y reservoir, reach several parts per billion (ppb) over polluted coastal/continental regions, with sub-ppb levels typical in more remote regions. Modeled annual mean surface [Cl] exhibits large spatial variability with the largest levels, typically in the range of $1\text{--}5 \times 10^4$ atoms cm^{-3} , in the polluted northern hemisphere. Chlorocarbon oxidation provides a tropospheric Cl_y source of up to ~ 4320 Gg Cl/yr, sustaining a background surface [Cl] of <0.1 to 0.5×10^3 atoms cm^{-3} over large areas. Globally, we estimate a tropospheric methane sink of $\sim 12\text{--}13$ Tg CH_4/yr due the $\text{CH}_4 + \text{Cl}$ reaction ($\sim 2.5\%$ of total CH_4 oxidation). Larger regional effects are predicted, with Cl accounting for ~ 10 to $>20\%$ of total boundary layer CH_4 oxidation in some locations.

1. Introduction

Atmospheric chlorine chemistry rose to prominence in the 1970s when it was discovered that Cl atoms, released from chlorofluorocarbons and other long-lived anthropogenic compounds, could catalyze ozone loss in the stratosphere [Molina and Rowland, 1974]. In contrast to the stratosphere, scientific understanding of chlorine sources/impacts in the troposphere, and the broader significance of halogen chemistry on tropospheric composition, has yet to be fully established [Saiz-Lopez and von Glasow, 2012; Simpson et al., 2015]. The importance of tropospheric chlorine is based primarily on the reactivity of Cl atoms toward various climate-relevant gases, including dimethyl sulfide, CH_4 , and other volatile organic compounds (VOCs). Rate constants for the reaction of Cl with a range of VOCs exceed those of analogous $\text{VOC} + \text{OH}$ reactions by up to several orders of magnitude [Atkinson et al., 2006], making atomic Cl a potentially important tropospheric oxidant. For example, several studies have shown that in high NO_x regions, peroxy radicals (e.g., HO_2 and others) produced from Cl-initiated VOC oxidation contribute to ozone production at the surface, which implicates chlorine chemistry in urban air pollution [e.g., Sarwar et al., 2012]. In addition, Lawler et al. [2011] have suggested that Cl atoms may account for up to 15% of CH_4 oxidation in certain regions.

Sources of tropospheric inorganic chlorine (Cl_y) are varied. Primary emissions of HCl occur from industrial activities, including coal combustion and incineration [McCulloch et al., 1999] and also from biomass burning [Lobert et al., 1999]. HCl is also released from sea-salt aerosol through acid displacement reactions involving

©2016. The Authors.

This is an open access article under the terms of the Creative Commons Attribution License, which permits use, distribution and reproduction in any medium, provided the original work is properly cited.

HNO_3 and H_2SO_4 [e.g., Eriksson, 1959]. More photolabile forms of Cl_y , such as gaseous Cl_2 and nitryl chloride (ClNO_2), may be produced from the oxidation of aerosol-bound chloride (Cl^- ; R1–3), as evidenced by numerous experimental studies [e.g., Finlayson-Pitts et al., 1989; Timonen et al., 1994; Caloz et al., 1996; Gebel and Finlayson-Pitts, 2001; Roberts et al., 2009], depending on local conditions. For example, Cl_2 production from R2 is expected to be efficient at low pH and is thereby most relevant on acidic particles.



Bromine and iodine may also play an important role in Cl^- activation within acidic aerosol solutions [e.g., Vogt et al., 1996, 1999] through hypohalous acids (HOX , where $X = \text{Cl}, \text{Br}, \text{I}$; R4).



In the marine boundary layer (MBL), where Cl^- in sea salt is abundant, production and photolysis of Cl_2 , ClNO_2 , BrCl , etc. provides a daytime Cl source. Significant Cl concentrations ($[\text{Cl}]$) may also be sustained through HCl oxidation, particularly in polluted coastal regions with elevated NO_x , despite the comparatively slow $\text{HCl} + \text{OH} \rightarrow \text{Cl} + \text{H}_2\text{O}$ reaction [e.g., Singh and Kasting, 1988; Keene et al., 2007; Pechtl and von Glasow, 2007]. As direct measurements of Cl in the troposphere have not yet been made, and because observations of Cl precursors are sparse, tropospheric $[\text{Cl}]$ is uncertain. Indirect methods have been used to infer typical MBL $[\text{Cl}]$ levels of $\sim 10^3$ to 10^5 atoms cm^{-3} [Saiz-Lopez and von Glasow, 2012, and references therein]. Better constraint on global $[\text{Cl}]$ is needed to fully determine the significance of chlorine chemistry on tropospheric composition. Notably, the global CH_4 sink due to Cl atom oxidation in the troposphere is poorly quantified. Current estimates, based on extrapolation of indirectly inferred regional $[\text{Cl}]$ levels, are in the range of 13–37 Tg CH_4/yr [Platt et al., 2004; Allan et al., 2007].

In addition to the above inorganic Cl precursors, chlorocarbons such as dichloromethane (CH_2Cl_2) and chloroform (CHCl_3) are present in the troposphere. These so-called very short lived substances (VSLSs) have, in recent years, been a major topic of stratospheric ozone-focused research, because industrial emissions of certain VSLS (not controlled by the UN Montreal Protocol) are increasing [e.g., Hossaini et al., 2015a]. Previous model studies that have included CH_2Cl_2 and CHCl_3 have assumed instantaneous release of Cl atoms upon initial source gas oxidation [e.g., Ordóñez et al., 2012; Schmidt et al., 2016]. However, various moderately stable and intermediate-organic product gases, most of which are subject to deposition processes, may be formed [Hossaini et al., 2015b]. The validity of this assumption is therefore unclear, and more broadly, the contribution of VSLS to tropospheric Cl_y is poorly quantified based on present-day VSLS loadings.

Motivated by the above, we have developed and implemented a chlorine chemistry scheme in the TOMCAT chemical transport model (CTM), incorporating the oxidation of chlorocarbons and a simplified treatment of sea-salt dechlorination. Simulations were performed to (i) examine the significance of VSLS as a tropospheric Cl_y source, (ii) compare tropospheric Cl_y production from organic versus inorganic sources, (iii) quantify tropospheric $[\text{Cl}]$, and (iv) estimate the contribution of Cl atoms to CH_4 oxidation. Simulations were also performed to test the sensitivity of $[\text{Cl}]$ to the choice and complexity of the chlorocarbon oxidation scheme. A description of TOMCAT is given in section 2.1. Section 2.2 details the chlorine scheme, including the sources and sinks of tropospheric Cl_y , gas-phase chemistry, and our simple treatment of sea-salt dechlorination. Results are presented in section 3 and conclusions given in section 4.

2. Model and Experiments

2.1. Chemical Transport Model

TOMCAT is a three-dimensional off-line CTM [Chipperfield, 2006] widely used for studies of tropospheric chemistry and transport [e.g., Monks et al., 2012; Richards et al., 2013]. The model runs off-line and uses prescribed 6 hourly wind, temperature, and humidity fields from the European Centre for Medium-Range Weather Forecasts ERA-Interim reanalysis [Dee et al., 2011]. The CTM includes a treatment of convection, described by Stockwell and Chipperfield [1999], and recently evaluated by Feng et al. [2011], based on the mass flux scheme of Tiedtke [1989]. In the boundary layer, turbulent mixing follows the non-local scheme

of *Holtslag and Boville* [1993]. For tracer advection, the CTM uses the conservation of second-order moment scheme of *Prather* [1986]. The CTM was run with a horizontal resolution of $\sim 2.8^\circ$ longitude by $\sim 2.8^\circ$ latitude and with 31 hybrid sigma-pressure (σ - p) levels (surface to ~ 30 km).

2.1.1. Benchmark Chemistry and Emissions

TOMCAT contains a comprehensive tropospheric chemistry scheme, including O_x - HO_x - NO_x - CO - CH_4 , C_2 - C_4 hydrocarbons [*Monks et al.*, 2016], bromine [*Breider et al.*, 2010, 2015], and iodine [*Breider*, 2010] chemistry. Photolysis rates are calculated online using the code of *Hough* [1988], which considers direct and scattered radiation, surface albedo, monthly mean climatological cloud fields, and ozone and temperature profiles. The model considers wet deposition of soluble gases in both convective and large-scale precipitation [*Giannakopoulos et al.*, 1999]. Dry deposition is calculated using diurnally and seasonally varying surface-type specific deposition velocities, with weighting applied by monthly land cover. Here the model used an extended degradation mechanism for VOCs, incorporating monoterpene oxidation, based on the Model for Ozone and Related chemical Tracers (MOZART, version 3) model [*Kinnison et al.*, 2007], and toluene, acetone, methanol, and acetaldehyde based on the Extended Tropospheric Chemistry scheme [*Folberth et al.*, 2006]. Isoprene oxidation follows the Mainz Isoprene Mechanism [*Pöschl et al.*, 2000]. This TOMCAT configuration is described and evaluated in *Monks et al.* [2016] and has been used previously to examine the tropospheric ozone budget [e.g., *Richards et al.*, 2013] and in several halogen-focused studies [e.g., *Hossaini et al.*, 2015b].

Surface emissions of anthropogenic NO_x , CO, and the aforementioned hydrocarbons are the same as those used in the POLar study using Aircraft, Remote Sensing, surface measurements and models of Climate, chemistry, Aerosols, and Transport (POLARCAT) Model Intercomparison Project [*Emmons et al.*, 2015]. These emissions are based on the Streets version 1.2 inventory [*Zhang et al.*, 2009], were updated for POLARCAT, and are appropriate for the year 2008. For biomass burning and natural wildfire emissions of these gases, data from the Global Fire Emissions Database version 3.1 [*van der Werf et al.*, 2006] were used, averaged over the 1997–2010 period. Natural isoprene and monoterpene emissions based on the Model of Emissions of Gases and Aerosols from Nature (version 2.1), as originally implemented by *Emmons et al.* [2010], were also used. All other natural emissions were prescribed from the POET data set [*Granier et al.*, 2005]. A common problem in global models is dealing with CH_4 which has a relatively long lifetime (~ 10 years) and therefore requires a very long spin-up time. To overcome this in TOMCAT, CH_4 is emitted and then scaled to give a surface global mean mixing ratio equal to 1800 ppb. Aircraft NO_x emissions were specified according to the Intergovernmental Panel on Climate Change Fifth Assessment Report data, and lightning NO_x production is parameterized based on cloud height and surface type.

2.1.2. Aerosol

TOMCAT calculates heterogeneous reaction rates according to *Jacob* [2000]. Aerosol surface areas, calculated from the aerosol size distribution, are supplied from the Global Model of Aerosol Processes (GLOMAP) aerosol microphysics model [*Spracklen et al.*, 2005]. The GLOMAP simulation used considered five aerosol components (sulfate, sea salt, black carbon, organic carbon, and dust). A recent description of the GLOMAP aerosol model is given in *Mann et al.* [2010]. Prescribed reactive uptake coefficients (γ) for heterogeneous reactions were taken from the literature. For N_2O_5 hydrolysis, γ for the aerosol types given above was calculated using the scheme of *Evans and Jacob* [2005], with the exception of dust, for which γ is based on *Mogili et al.* [2006]. Most relevant to this study are heterogeneous reactions involving sea salt, which liberates particulate chloride into the gas phase and constitutes a net source of Cl_y (see section 2.2.2).

2.1.3. Bromine and Iodine Simulations

TOMCAT includes a treatment of bromine and iodine chemistry (coupled to Cl through species such as BrCl and ICl and reactions of ClO with BrO and IO). The bromine scheme was described and evaluated by *Breider et al.* [2010, 2015] and has been shown to provide a good simulation of measured BrO at various sites. Briefly, it considers bromine release from explicit sea-salt emissions, based on the parameterization of *Yang et al.* [2005]. This parameterization incorporates observed size-dependent bromide depletion factors in sea-salt aerosol [*Sander et al.*, 2003] and, in TOMCAT, is extended to account for the effects of aerosol acidification [*Alexander et al.*, 2005]. In addition, TOMCAT considers oceanic emissions of the brominated VSLs, $CHBr_3$, CH_2Br_2 , $CHBr_2Cl$, CH_2BrCl , and $CHBrCl_2$ [e.g., *Hossaini et al.*, 2013], some of which constitute a source of chlorine (see section 2.2.1). TOMCAT also includes a comprehensive treatment of tropospheric iodine including all major I_y species; gas-phase chemistry; heterogeneous recycling of HOI, INO_2 , and $IONO_2$ on aerosol; and production/loss of higher iodine oxides (e.g., I_2O_2 and I_2O_4), following *Saiz-Lopez et al.* [2014]. Ocean

emissions of various iodine-containing VSLS (e.g., CH_3I , CH_2I_2 , CH_2ICl , and CH_2IBr), along with a parameterization of oceanic emissions of HOI and I_2 [Carpenter *et al.*, 2013; MacDonald *et al.*, 2014], are considered. Emissions of the halogenated VSLS are prescribed from the global inventories of Ordóñez *et al.* [2012], with the exception of CHBr_3 which uses the Ziska *et al.* [2013] inventory. This model configuration has been shown to provide good agreement to a range of VSLS observations [e.g., Hossaini *et al.*, 2013, 2016].

2.2. Chlorine Sources and Chemistry

Building on Hossaini *et al.* [2015b], a chlorine chemistry scheme has been developed and implemented in TOMCAT. The scheme includes 10 Cl_y species (Cl , ClO , OCIO , Cl_2 , HCl , HOCl , ClONO_2 , ClNO_2 , BrCl , and ICl) that participate in more than 40 gas-phase reactions (Table 1). The Cl_y scheme is a reduced reaction mechanism formulated from the more detailed reaction mechanism of the 1-D MISTRA model [e.g., von Glasow *et al.*, 2002]. It incorporates the Cl atom oxidation of alkanes (CH_4 , C_2H_6 , C_3H_8 , and C_4H_{10}), aldehydes (HCHO , CH_3CHO , and $\text{C}_2\text{H}_5\text{CHO}$), and other organic compounds. Reactions of Cl atoms with alkenes, which generally proceed through chlorine addition, are not considered. Kinetic data were taken from International Union of Pure and Applied Chemistry or NASA Jet Propulsion Laboratory data evaluations [Atkinson *et al.*, 2006, 2007, 2008; Sander *et al.*, 2011; Burkholder *et al.*, 2015], where available. Otherwise, kinetic data from the Master Chemical Mechanism (MCM; version 3.3.1) were used (<http://mcm.leeds.ac.uk/MCM/>). Several Cl_y species are subject to wet and/or dry deposition in TOMCAT (Table 2). Henry's law data were taken from Sander [2015], where possible. Estimated dry deposition velocities were taken from Ordóñez *et al.* [2012].

Sources of tropospheric chlorine in TOMCAT include chlorocarbons, for which a detailed oxidation scheme is described in section 2.2.1, and sea-salt dechlorination; our simplified treatment of which is described in section 2.2.2. The model also considers primary HCl emissions from industry [McCulloch *et al.*, 1999] and biomass burning [Lobert *et al.*, 1999], which provide ~ 6.6 and ~ 6.4 Tg Cl/yr , respectively. We make an upper limit assumption that all chlorine emitted from biomass burning occurs as HCl . Note that the HCl emission inventories were developed in the late 1990s and in the absence of more recent global data should be considered uncertain.

2.2.1. Organic Chlorine Sources

Ten chlorocarbons are included in this tropospheric TOMCAT configuration. This includes the five VSLS CH_2Cl_2 , CHCl_3 , tetrachloroethene (C_2Cl_4), trichloroethene (C_2HCl_3), and 1,2-dichloroethane ($\text{CH}_2\text{ClCH}_2\text{Cl}$). With the exception of CHCl_3 , emissions of these VSLS are dominated by anthropogenic sources. Following Hossaini *et al.* [2015b], a latitude-dependent surface boundary condition for these VSLS was prescribed, based on 2014 surface measurements from the National Oceanic and Atmospheric Administration (NOAA) and Advanced Global Atmospheric Gases Experiment (AGAGE) monitoring networks. Surface volume mixing ratios (VMRs) were assigned in five latitude bands ($>60^\circ\text{N}$, $30\text{--}60^\circ\text{N}$, $0\text{--}30^\circ\text{N}$, $0\text{--}30^\circ\text{S}$, and $>30^\circ\text{S}$) and are summarized in Table 3. As recent surface measurements of $\text{CH}_2\text{ClCH}_2\text{Cl}$ and C_2HCl_3 are not available from the above networks, their latitude-dependent surface VMR was prescribed from boundary layer measurements obtained during the 2009–2011 HIPPO aircraft mission [Wofsy *et al.*, 2011]. TOMCAT also considers the relatively long-lived source gas, methyl chloride (CH_3Cl), constrained at the surface in a similar fashion. For the natural ocean-emitted VSLS CHBrCl_2 , CHBr_2Cl , CH_2BrCl , and CH_2ICl we used the top-down global emissions inventory from Ordóñez *et al.*, 2012, instead of imposing a surface mixing ratio boundary condition. This inventory considers the varying geographical distribution of the sea-to-air flux of these compounds, with emissions weighted in the tropics toward observed chlorophyll *a* concentrations and with hemispheric latitudinal dependent distributions between 20 and 50°N/S as well as above 50°N/S . The annual mean surface VMR of these VSLS in TOMCAT is also shown in Table 3.

Most previous model studies have assumed an instantaneous release of all Cl atoms in a molecule, upon chlorocarbon oxidation [e.g., Ordóñez *et al.*, 2012]. For the relatively minor (least abundant) naturally emitted VSLS CHBrCl_2 , CHBr_2Cl , CH_2BrCl , and CH_2ICl , this approach is also adopted here. However, we have implemented a detailed tropospheric degradation scheme in TOMCAT for the more abundant chlorine-containing gases CH_3Cl , CH_2Cl_2 , CHCl_3 , and $\text{CH}_2\text{ClCH}_2\text{Cl}$ that consider organic product gases (Table 4). Oxidation of the above chlorocarbon source gases share a number of common steps, with loss proceeding via hydrogen abstraction following reaction with OH or Cl (G53–60; Table 4). The initial radical products (CH_2Cl , CHCl_2 , CCl_3 , and CH_2ClCHCl) are rapidly oxidized under tropospheric conditions to peroxy radicals (i.e., CH_2ClO_2 , CHCl_2O_2 , CCl_3O_2 , and $\text{CH}_2\text{ClCHClO}_2$, respectively). These peroxy radicals may react with NO , HO_2 , other peroxy species

Table 1. Reactions and Kinetic Data for the TOMCAT Inorganic Chlorine Chemistry Scheme

Number	Reaction	Rate Constant ^a	Reference ^b
Bimolecular			
G1	Cl + O ₃ → ClO + O ₂	$2.3 \times 10^{-11} \exp(-200/T)$	JPL15
G2	ClO + HO ₂ → HOCl + O ₂	$2.6 \times 10^{-12} \exp(290/T)$	JPL15
G3	Cl + HO ₂ → HCl + O ₂	$1.4 \times 10^{-11} \exp(270/T)$	JPL15
G4	Cl + HO ₂ → ClO + OH	$3.6 \times 10^{-11} \exp(-375/T)$	JPL15
G5	HCl + OH → Cl + H ₂ O	$1.8 \times 10^{-12} \exp(-250/T)$	JPL15
G6	ClO + NO → Cl + NO ₂	$6.4 \times 10^{-12} \exp(290/T)$	JPL15
G7	ClO + ClO → Cl + Cl + O ₂	$3.0 \times 10^{-11} \exp(-2450/T)$	JPL15
G8	ClO + ClO → Cl ₂ + O ₂	$1.0 \times 10^{-12} \exp(-1590/T)$	JPL15
G9	Cl ₂ + OH → HOCl + Cl	$2.6 \times 10^{-12} \exp(-1100/T)$	JPL15
G10	ClO + OH → Cl + HO ₂	$7.4 \times 10^{-12} \exp(270/T)$	JPL15
G11	ClO + IO → ICl + O ₂	$0.2 \times 4.7 \times 10^{-12} \exp(280/T)$	IUPAC
G12	ClO + IO → Cl + I + O ₂	$0.25 \times 4.7 \times 10^{-12} \exp(280/T)$	IUPAC
G13	ClO + IO → OCIO + I	$0.55 \times 4.7 \times 10^{-12} \exp(280/T)$	IUPAC
G14	ClO + BrO → OCIO + Br	$1.6 \times 10^{-12} \exp(430/T)$	IUPAC
G15	ClO + BrO → Br + Cl + O ₂	$2.9 \times 10^{-12} \exp(220/T)$	IUPAC
G16	ClO + BrO → BrCl + O ₂	$5.8 \times 10^{-13} \exp(170/T)$	IUPAC
G17	HOCl + OH → ClO + H ₂ O	$3.0 \times 10^{-12} \exp(-500/T)$	JPL15
G18	ClONO ₂ + OH → HOCl + NO ₃	$1.2 \times 10^{-12} \exp(-330/T)$	IUPAC
G19	ClONO ₂ + Cl → Cl ₂ + NO ₃	$6.2 \times 10^{-12} \exp(145/T)$	IUPAC
G20	ClNO ₂ + OH → HOCl + NO ₂	$2.4 \times 10^{-12} \exp(-1250/T)$	IUPAC
G21	Cl + CH ₄ + O ₂ → HCl + CH ₃ O ₂	$7.3 \times 10^{-12} \exp(-1280/T)$	JPL11
G22	Cl + C ₂ H ₆ → HCl + EtOO	$7.2 \times 10^{-11} \exp(-70/T)$	JPL15
G23	Cl + C ₃ H ₈ → HCl + n-C ₃ H ₇ O ₂	$6.54 \times 10^{-11} \exp(60/T)$	JPL15
G24	Cl + C ₃ H ₈ → HCl + i-C ₃ H ₇ O ₂	$8.12 \times 10^{-11} \exp(-90/T)$	JPL15
G25	Cl + C ₄ H ₁₀ → HCl + C ₄ H ₉ O ₂	2.05×10^{-10}	IUPAC
G26	Cl + HCHO (+O ₂) → HCl + HO ₂ + CO	$8.1 \times 10^{-11} \exp(-30/T)$	JPL15
G27	Cl + CH ₃ CHO (+O ₂) → HCl + CH ₃ CO ₃	8.0×10^{-11}	IUPAC
G28	Cl + EtCHO → HCl + EtCO ₃	1.3×10^{-10}	IUPAC
G29	Cl + CH ₃ OH (+O ₂) → HCl + HO ₂ + HCHO	5.5×10^{-11}	JPL15
G30	Cl + CH ₃ OOH → HCl + HCHO + OH	5.9×10^{-11}	IUPAC
G31	Cl + MeCO ₂ H → HCl + MeO ₂	2.65×10^{-14}	IUPAC
G32	Cl + HCOOH → HCl + HO ₂	1.9×10^{-13}	IUPAC
G33	Cl + CH ₃ NO ₃ → HCl + HCHO + NO ₂	2.4×10^{-13}	IUPAC
G34	ClO + CH ₃ O ₂ (+O ₂) → Cl + HCHO + HO ₂ + O ₂	$3.3 \times 10^{-12} \exp(-115/T)$	JPL11
G35	Cl + (CH ₃) ₂ S → products	3.3×10^{-10}	IUPAC
Termolecular			
G36	ClO + NO ₂ + M → ClONO ₂ + M	$k_0 = 1.8 \times 10^{-31} (T/300)^{-3.4} k_{inf} = 1.5 \times 10^{-11} (T/300)^{-1.9}$	JPL15
G37	Cl + NO ₂ + M → ClNO ₂ + M	$k_0 = 1.8 \times 10^{-31} (T/300)^{-2.0} k_{inf} = 1.0 \times 10^{-10} (T/300)^{-1.0}$	JPL15
Photolysis			
G38	ClO + hv → Cl + O(³ P)	c	JPL11
G39	HOCl + hv → Cl + OH	c	JPL11
G40	ClONO ₂ + hv → ClO + NO ₂	c	JPL11
G41	ClONO ₂ + hv → Cl + NO ₃	c	JPL11
G42	ClNO ₂ + hv → Cl + NO ₂	c	JPL11
G43	Cl ₂ + hv → Cl + Cl	c	JPL11
G44	OCIO + hv → ClO + O(³ P)	c	JPL11
G45	BrCl + hv → Br + Cl	c	JPL11
G46	ICl + hv → I + Cl	c	JPL11

^aRate constant units: bimolecular (cm³ molecules⁻¹ s⁻¹), termolecular (k₀ units: cm⁶ molecules⁻² s⁻¹, k_{inf} units: cm³ molecules⁻¹ s⁻¹).

^bJPL11 [Sander et al., 2011], JPL15 [Burkholder et al., 2015], and IUPAC [Atkinson et al., 2004, 2007].

^cAbsorption cross sections from reference.

(e.g., CH₃O₂), or with themselves [e.g., Catoire et al., 1996; Biggs et al., 1999]. The expected major organic products from oxidation of the above source gases are (i) phosgene (CCl₂O), following CHCl₃ oxidation, and (ii) formyl chloride (CHClO), following CH₃Cl, CH₂Cl₂, and CH₂ClCH₂Cl oxidation [e.g., Catoire et al., 1997; Bilde et al., 1999; Ko et al., 2003]. In the troposphere, CCl₂O is long lived against gas-phase oxidation

Table 2. Henry's Constants (K_H) Used to Calculate Wet Deposition Rates^a

Species	K_H (M/atm)	$-\Delta_{\text{soln}}H/R$ (K)	Reference
HCl	1.2 ^b	9001	<i>Brimblecombe and Clegg</i> [1988]
HOCl	670	5862	<i>Huthwelker et al.</i> [1995]
Cl ₂	0.086	2000	<i>Kavanaugh and Trussell</i> [1980]
ClONO ₂	∞	-	<i>Sander</i> [2015]
ClNO ₂	0.024	-	<i>Behnke et al.</i> [1997]
BrCl	0.94	5600	<i>Bartlett and Margerum</i> [1999]
ICl	110	5600 ^c	<i>Wagman et al.</i> [1982]
CH ₂ ClOOH	2.5×10^{3c}	-	<i>Krysztofiak et al.</i> [2012]
CHCl ₂ OOH	2.2×10^{4c}	-	<i>Krysztofiak et al.</i> [2012]
CCl ₃ OOH	1.9×10^{5c}	-	<i>Krysztofiak et al.</i> [2012]
CH ₂ ClOH	2.0×10^{3c}	-	<i>Krysztofiak et al.</i> [2012]
CHCl ₂ OH	1.7×10^{4c}	-	<i>Krysztofiak et al.</i> [2012]
CCl ₃ OH	1.5×10^{5c}	-	<i>Krysztofiak et al.</i> [2012]
CHClO	74.0 ^c	-	<i>Krysztofiak et al.</i> [2012]
CCl ₂ O	0.059	3800	<i>de Bruyn et al.</i> [1995]

^aThe enthalpy of solution ($\Delta_{\text{soln}}H$) is used to describe the temperature dependence of K_H [e.g., *Sander*, 2015].

^bConsidering acid dissociation constant of 1.7×10^6 .

^cAssume the value from analogous brominated compound.

and is not readily photolyzed at wavelengths available in the troposphere. Its residence time is estimated to be ~70 days, with hydrolysis in cloud water being the principal sink [*Kindler et al.*, 1995]. The atmospheric fate of CHClO is uncertain. Its reaction with OH has a rate constant of $<5 \times 10^{-13} \text{ cm}^3 \text{ molecules}^{-1} \text{ s}^{-1}$ at 300 K, and its photolysis rate is on the order of $1 \times 10^{-8} \text{ s}^{-1}$ at 5 km altitude [*Ko et al.*, 2003]. We assumed a CHClO Henry's law constant (based on analogous bromine species) of 74 M/atm. This order of magnitude seems reasonable compared to other carbonyl compounds [e.g., *Zhou and Mopper*, 1990]. Large Henry's law constants for a number of chlorinated organic products suggest that

wet deposition could provide an efficient sink for these compounds (Table 2).

2.2.2. Sea-Salt Dechlorination and Recycling of Cl_y

A number of heterogeneous reactions involving chlorine were implemented in TOMCAT, including the hydrolysis of ClONO₂ on sea-salt (SS) and sulfate (SUL) aerosols:



Recycling of Cl_y species and SS dechlorination occur through several heterogeneous reactions involving chlorine, bromine, iodine, and odd nitrogen species. Such reactions provide a net source of tropospheric Cl_y (particularly to the MBL) in the form of Cl₂, BrCl, ICl, ClONO₂, and HCl [e.g., *Vogt et al.*, 1999; *Sander et al.*, 1999]. Our approach to implementing these reactions follows that of recent Community Atmosphere

Table 3. Chlorocarbons in TOMCAT and Their Surface Boundary Condition^a

Chlorocarbon	Formula	Latitude Band ^b					Origin ^c	Lifetime ^d (Days)
		>60°N	30–60°N	0–30°N	0–30°S	<30°S		
Methyl chloride	CH ₃ Cl	518.6	545.1	571.6	551.8	522.0	N(A)	573
Dichloromethane	CH ₂ Cl ₂	60.6	63.3	56.1	20.0	17.0	A(N)	109
Chloroform	CHCl ₃	13.0	8.6	6.7	5.4	5.7	N(A)	112
Tetrachloroethene	C ₂ Cl ₄	2.3	3.4	1.7	0.6	0.5	A	67
Trichloroethene	C ₂ HCl ₃	0.5	0.5	0.5	0.2	0.2	A	5
1,2-Dichloroethane	CH ₂ ClCH ₂ Cl	15.0	15.0	10.0	3.0	2.0	A	47
Bromodichloromethane ^e	CHBrCl ₂	0.14	0.16	0.17	0.13	0.08	N	41
Dibromochloromethane ^e	CHBr ₂ Cl	0.06	0.06	0.1	0.1	0.07	N	32
Bromochloromethane ^e	CH ₂ BrCl	0.18	0.19	0.23	0.22	0.19	N	103
Chloriodomethane ^e	CH ₂ ICl	0.03	0.06	0.11	0.09	0.03	N	0.1

^aExpressed as a latitude-dependent volume mixing ratio (ppt). See main text.

^bCH₃Cl, CH₂Cl₂, CHCl₃, and C₂Cl₄ from surface observations of the NOAA and AGAGE global monitoring networks in 2014. C₂HCl₃ and CH₂ClCH₂Cl from boundary layer observations during HIPPO aircraft mission (2009–2011). See main text.

^c"A" denotes anthropogenic origin, "N" natural origin "A(N)" predominately anthropogenic with minor natural source, and "N(A)" predominately natural with relatively minor anthropogenic source.

^dCH₃Cl, lifetime with respect to OH oxidation in the troposphere. VLSL, annual mean local lifetime (against OH oxidation and photolysis) appropriate for the tropical (25°N–25°S) boundary layer [*Carpenter et al.*, 2014]. CH₂Cl lifetime from *Ko et al.* [2003].

^eCHBrCl₂, CHBr₂Cl, CH₂BrCl, and CH₂ICl are emitted using the top-down inventory of *Ordóñez et al.* [2012]. Modeled annual mean surface mixing ratios within each latitude band are shown for comparison with the other species.

Table 4. Reactions and Kinetic Data in TOMCAT's Tropospheric Degradation Scheme for Chlorocarbons^a

Number	Reaction ^b	Rate Constant ^c	Notes	Reference
Loss of chlorinated source gases				
G47	$\text{CHBrCl}_2 + \text{OH} \rightarrow \text{Br} + 2\text{Cl} + \text{H}_2\text{O}$	$9.4 \times 10^{-13} \exp(-510/T)$	-	JPL15
G48	$\text{CHBrCl}_2 + \text{h}\nu \rightarrow \text{Br} + 2\text{Cl}$	-	-	JPL11
G49	$\text{CHBr}_2\text{Cl} + \text{OH} \rightarrow 2\text{Br} + \text{Cl} + \text{H}_2\text{O}$	$9.0 \times 10^{-13} \exp(-420/T)$	-	JPL15
G50	$\text{CHBr}_2\text{Cl} + \text{h}\nu \rightarrow 2\text{Br} + \text{Cl}$	-	-	JPL11
G51	$\text{CH}_2\text{BrCl} + \text{OH} \rightarrow \text{Br} + \text{Cl} + \text{H}_2\text{O}$	$2.4 \times 10^{-12} \exp(920/T)$	-	JPL11
G52	$\text{CH}_2\text{ICl} + \text{h}\nu \rightarrow \text{I} + \text{Cl}$	-	-	JPL11
G53	$\text{CH}_3\text{Cl} + \text{OH} + \text{O}_2 \rightarrow \text{CH}_2\text{ClO}_2 + \text{H}_2\text{O}$	$2.1 \times 10^{-12} \exp(-1210/T)$	d	IUPAC
G54	$\text{CH}_3\text{Cl} + \text{Cl} + \text{O}_2 \rightarrow \text{CH}_2\text{ClO}_2 + \text{HCl}$	$1.8 \times 10^{-11} \exp(-1081/T)$	d	IUPAC
G55	$\text{CH}_2\text{Cl}_2 + \text{OH} + \text{O}_2 \rightarrow \text{CHCl}_2\text{O}_2 + \text{H}_2\text{O}$	$1.8 \times 10^{-12} \exp(-860/T)$	d	IUPAC
G56	$\text{CH}_2\text{Cl}_2 + \text{Cl} + \text{O}_2 \rightarrow \text{CHCl}_2\text{O}_2 + \text{HCl}$	$5.9 \times 10^{-12} \exp(-850/T)$	d	IUPAC
G57	$\text{CHCl}_3 + \text{OH} + \text{O}_2 \rightarrow \text{CCl}_3\text{O}_2 + \text{H}_2\text{O}$	$1.8 \times 10^{-12} \exp(-850/T)$	d	IUPAC
G58	$\text{CHCl}_3 + \text{Cl} + \text{O}_2 \rightarrow \text{CCl}_3\text{O}_2 + \text{HCl}$	$2.4 \times 10^{-12} \exp(-920/T)$	d	IUPAC
G59	$\text{CH}_2\text{ClCH}_2\text{Cl} + \text{OH} + \text{O}_2 \rightarrow \text{CH}_2\text{ClCHClO}_2 + \text{H}_2\text{O}$	$8.7 \times 10^{-12} \exp(-1070/T)$	d	IUPAC
G60	$\text{CH}_2\text{ClCH}_2\text{Cl} + \text{Cl} + \text{O}_2 \rightarrow \text{CH}_2\text{ClCHClO}_2 + \text{HCl}$	1.3×10^{-12}	d	j
G61	$\text{C}_2\text{Cl}_4 + \text{OH} + \text{O}_2 \rightarrow \text{C}_2\text{Cl}_4(\text{OH})\text{O}_2$	$3.5 \times 10^{-12} \exp(-920/T)$	d	IUPAC
G62	$\text{C}_2\text{Cl}_4 + \text{Cl} + \text{M} + \text{O}_2 \rightarrow \text{C}_2\text{Cl}_5\text{O}_2 + \text{M}$	$k_0 = 1.4 \times 10^{-28} (T/300)^{-8.5} k_{\text{inf}} = 4.0 \times 10^{-11} (T/300)^{-1.2}$	d	JPL15
G63	$\text{C}_2\text{HCl}_3 + \text{OH} \rightarrow \text{C}_2\text{HCl}_3(\text{OH})\text{O}_2$	$3.0 \times 10^{-13} \exp(565/T)$	d	IUPAC
G64	$\text{C}_2\text{HCl}_3 + \text{Cl} + \text{O}_2 \rightarrow \text{C}_2\text{HCl}_4\text{O}_2$	7.2×10^{-11}	d	k
Loss of chlorinated peroxy radicals				
G65	$\text{CH}_2\text{ClO}_2 + \text{NO} \rightarrow \text{CH}_2\text{ClO} + \text{NO}_2$	$7.0 \times 10^{-12} \exp(300/T)$	e	JPL15
G66	$\text{CH}_2\text{ClO}_2 + \text{NO}_3 \rightarrow \text{CH}_2\text{ClO} + \text{NO}_2 + \text{O}_2$	2.3×10^{-12}	e	MCM
G67	$\text{CH}_2\text{ClO}_2 + \text{HO}_2 \rightarrow \text{CH}_2\text{ClOOH} + \text{O}_2$	$3.2 \times 10^{-13} \exp(820/T)$	0.3	IUPAC
G68	$\text{CH}_2\text{ClO}_2 + \text{HO}_2 \rightarrow \text{CHClO} + \text{H}_2\text{O} + \text{O}_2$	$3.2 \times 10^{-13} \exp(820/T)$	0.7	IUPAC
G69	$\text{CH}_2\text{ClO}_2 + \text{CH}_3\text{O}_2 + \text{O}_2 \rightarrow \text{CH}_2\text{ClO} + \text{HCHO} + \text{HO}_2 + 2\text{O}_2$	2.5×10^{-12}	0.6	IUPAC
G70	$\text{CH}_2\text{ClO}_2 + \text{CH}_3\text{O}_2 \rightarrow \text{CH}_2\text{ClOH} + \text{HCHO} + \text{O}_2$	2.5×10^{-12}	0.2	IUPAC
G71	$\text{CH}_2\text{ClO}_2 + \text{CH}_3\text{O}_2 \rightarrow \text{CHClO} + \text{CH}_3\text{OH} + \text{O}_2$	2.5×10^{-12}	0.2	IUPAC
G72	$\text{CH}_2\text{ClO}_2 + \text{CH}_2\text{ClO}_2 \rightarrow 2\text{CH}_2\text{ClO} + \text{O}_2$	$1.9 \times 10^{-13} \exp(870/T)$	-	IUPAC
G73	$\text{CHCl}_2\text{O}_2 + \text{NO} \rightarrow \text{CHCl}_2\text{O} + \text{NO}_2$	$4.0 \times 10^{-12} \exp(360/T)$	e	MCM
G74	$\text{CHCl}_2\text{O}_2 + \text{NO}_3 \rightarrow \text{CHCl}_2\text{O} + \text{NO}_2$	2.3×10^{-12}	e	MCM
G75	$\text{CHCl}_2\text{O}_2 + \text{HO}_2 \rightarrow \text{CHCl}_2\text{OOH} + \text{O}_2$	$5.6 \times 10^{-13} \exp(700/T)$	0.0	IUPAC
G76	$\text{CHCl}_2\text{O}_2 + \text{HO}_2 \rightarrow \text{CCl}_2\text{O} + \text{H}_2\text{O} + \text{O}_2$	$5.6 \times 10^{-13} \exp(700/T)$	0.7	IUPAC
G77	$\text{CHCl}_2\text{O}_2 + \text{HO}_2 \rightarrow \text{CHClO} + \text{HOCl} + \text{O}_2$	$5.6 \times 10^{-13} \exp(700/T)$	0.3	IUPAC
G78	$\text{CHCl}_2\text{O}_2 + \text{CH}_3\text{O}_2 \rightarrow \text{CHCl}_2\text{O} + \text{HCHO} + \text{HO}_2$	2.0×10^{-12}	0.6	MCM
G79	$\text{CHCl}_2\text{O}_2 + \text{CH}_3\text{O}_2 \rightarrow \text{CHCl}_2\text{OH} + \text{HCHO} + \text{O}_2$	2.0×10^{-12}	0.2	MCM
G80	$\text{CHCl}_2\text{O}_2 + \text{CH}_3\text{O}_2 \rightarrow \text{CCl}_2\text{O} + \text{CH}_3\text{OH} + \text{O}_2$	2.0×10^{-12}	0.2	MCM
G81	$\text{CHCl}_2\text{O}_2 + \text{CHCl}_2\text{O}_2 \rightarrow 2\text{CHCl}_2\text{O} + \text{O}_2$	7.0×10^{-12}	-	l
G82	$\text{CCl}_3\text{O}_2 + \text{NO} \rightarrow \text{CCl}_3\text{O} + \text{NO}_2$	$7.3 \times 10^{-12} \exp(270/T)$	e	JPL15
G83	$\text{CCl}_3\text{O}_2 + \text{NO}_3 \rightarrow \text{CCl}_3\text{O} + \text{NO}_2 + \text{O}_2$	2.3×10^{-12}	e	MCM
G84	$\text{CCl}_3\text{O}_2 + \text{HO}_2 \rightarrow \text{CCl}_3\text{OOH} + \text{O}_2$	$4.7 \times 10^{-13} \exp(710/T)$	0.0	IUPAC
G85	$\text{CCl}_3\text{O}_2 + \text{HO}_2 \rightarrow \text{CCl}_2\text{O} + \text{HOCl} + \text{O}_2$	$4.7 \times 10^{-13} \exp(710/T)$	1.0	IUPAC
G86	$\text{CCl}_3\text{O}_2 + \text{CH}_3\text{O}_2 \rightarrow \text{CCl}_3\text{O} + \text{CH}_3\text{O} + \text{O}_2$	6.6×10^{-12}	0.5	IUPAC
G87	$\text{CCl}_3\text{O}_2 + \text{CH}_3\text{O}_2 \rightarrow \text{CCl}_3\text{OH} + \text{HCHO} + \text{O}_2$	6.6×10^{-12}	0.5	IUPAC
G88	$\text{CCl}_3\text{O}_2 + \text{CCl}_3\text{O}_2 \rightarrow 2\text{CCl}_3\text{O} + \text{O}_2$	$3.3 \times 10^{-13} \exp(740/T)$	-	IUPAC
G89	$\text{CH}_2\text{ClCHClO}_2 + \text{NO} + \text{O}_2 \rightarrow \text{CH}_2\text{ClO}_2 + \text{HCl} + \text{CO} + \text{NO}_2$	9.0×10^{-12}	f	j
G90	$\text{C}_2\text{Cl}_4(\text{OH})\text{O}_2 + \text{NO} \rightarrow \text{CCl}_3\text{O}_2 + \text{Cl} + \text{NO}_2 + \text{OH}$	$4.0 \times 10^{-12} \exp(360/T)$	g	MCM
G91	$\text{C}_2\text{Cl}_4(\text{OH})\text{O}_2 + \text{NO}_3 \rightarrow \text{CCl}_3\text{O}_2 + \text{Cl} + \text{NO}_2 + \text{OH}$	2.3×10^{-12}	g	MCM
G92	$\text{C}_2\text{Cl}_5\text{O}_2 + \text{NO} \rightarrow \text{CCl}_3\text{O}_2 + 2\text{Cl} + \text{NO}_2$	6.2×10^{-12}	g	m
G93	$\text{C}_2\text{HCl}_3(\text{OH})\text{O}_2 + \text{NO} + \text{O}_2 \rightarrow \text{CHClO} + \text{COCl}_2 + \text{HO}_2 + \text{NO}_2$	$4.0 \times 10^{-12} \exp(360/T)$	h	MCM
G94	$\text{C}_2\text{HCl}_4\text{O}_2 + \text{NO} + \text{O}_2 \rightarrow \text{CHClO} + \text{CCl}_3\text{O}_2 + \text{NO}_2$	$4.0 \times 10^{-12} \exp(360/T)$	h	MCM
Loss of chlorinated hydroperoxides				
G95	$\text{CH}_2\text{ClOOH} + \text{OH} \rightarrow \text{CH}_2\text{ClO}_2 + \text{H}_2\text{O}$	$1.9 \times 10^{-12} \exp(190/T)$	-	MCM
G96	$\text{CH}_2\text{ClOOH} + \text{h}\nu \rightarrow \text{CH}_2\text{ClO} + \text{OH}$	-	i	JPL
G97	$\text{CHCl}_2\text{OOH} + \text{OH} \rightarrow \text{CHCl}_2\text{O}_2 + \text{H}_2\text{O}$	$1.9 \times 10^{-12} \exp(190/T)$	-	MCM
G98	$\text{CHCl}_2\text{OOH} + \text{h}\nu \rightarrow \text{CHCl}_2\text{O} + \text{OH}$	-	i	JPL11
G99	$\text{CCl}_3\text{OOH} + \text{OH} \rightarrow \text{CCl}_3\text{O}_2 + \text{H}_2\text{O}$	$1.9 \times 10^{-12} \exp(190/T)$	-	MCM
G100	$\text{CCl}_3\text{OOH} + \text{h}\nu \rightarrow \text{CCl}_3\text{O} + \text{OH}$	-	i	JPL11
Loss of chlorinated alcohols				
G101	$\text{CH}_2\text{ClOH} + \text{OH} \rightarrow \text{CHClO} + \text{HO}_2 + \text{H}_2\text{O}$	1.08×10^{-12}	-	MCM
G102	$\text{CHCl}_2\text{OH} + \text{OH} + \text{O}_2 \rightarrow \text{CCl}_2\text{O} + \text{HO}_2 + \text{H}_2\text{O}$	9.34×10^{-13}	-	MCM
G103	$\text{CCl}_3\text{OH} + \text{OH} \rightarrow \text{CCl}_3\text{O} + \text{H}_2\text{O}$	3.6×10^{-14}	-	MCM

Table 4. (continued)

Number	Reaction ^b	Rate Constant ^c	Notes	Reference
Loss of chlorinated carbonyls				
G104	CHClO + OH → Cl + CO + H ₂ O	3.2×10^{-13}	-	IUPAC
G105	CHClO + Cl → HCl + Cl + CO	$8.1 \times 10^{-12} \exp(-710/T)$	-	IUPAC
G106	CHClO + NO ₃ → Cl + CO + HNO ₃	$1.4 \times 10^{-12} \exp(-1860/T)$	-	MCM
G107	CHClO + hv + O ₂ → Cl + CO + HO ₂	-	-	JPL11
G108	CCl ₂ O + OH → 2Cl + OH + CO	5.0×10^{-15}	-	IUPAC
G109	CCl ₂ O + O(¹ D) → Cl + ClO + CO	$2.2 \times 10^{-12} \exp(30/T)$	-	JPL11
G110	CCl ₂ O + hv → 2Cl + CO	-	-	JPL11

^aBranching ratios where applicable are given in the Notes column.

^bFor some reactions a full balance in terms of C atoms is not easily achieved and is therefore neglected.

^cRate constant units: bimolecular (cm³ molecules⁻¹ s⁻¹), termolecular (k_0 units: cm⁶ molecules⁻² s⁻¹, k_{inf} units: cm³ molecules⁻¹ s⁻¹).

^dH abstraction (G53–G60). Cl/OH addition (G61–G64). Initial products (CH₂Cl, CHCl₂, CCl₃, etc.) add O₂ rapidly.

^eAssumed instantaneous: CH₂ClO + O₂ → CHClO + HO₂, CHCl₂O → CHClO + Cl, and CCl₃O → CCl₂O + Cl.

^fBased on HCl elimination mechanism outlined in Wallington *et al.* [1996].

^gAssumed products based on ab initio study of Christiansen and Francisco [2010a] and consistent with experimentally observed end products of CCl₄ oxidation [e.g., Thüner *et al.*, 1999].

^hAssumed products based on ab initio study of Christiansen and Francisco [2010b] and consistent with experimentally observed end products of C₂HCl₃ oxidation [e.g., Catoire *et al.*, 1997].

ⁱPhotolysis rates calculated assuming absorption cross sections of CH₃OOH.

^jWallington *et al.* [1996].

^kCatoire *et al.* [1997].

^lBiggs *et al.* [1999].

^mOlkhov and Smith [2004].

Model with Chemistry (CAM-Chem) model studies [Fernandez *et al.*, 2014; Saiz-Lopez *et al.*, 2014], whereby it is assumed that (i) the rate-limiting step of the chlorine recycling process is the uptake of the gaseous reactant to the aerosol surface and (ii) that the concentration of SS chloride is sufficient to enable the heterogeneous reaction to proceed until the aerosol is physically removed by deposition processes. A summary of SS dechlorination reactions and prescribed reactive uptake coefficients (γ values) are given in Table 5.

A particular focus of recent research has been on the role of N₂O₅ in chlorine activation. Several experimental studies have observed production of ClNO₂ following the uptake of N₂O₅ onto deliquesced SS droplets [e.g., Stewart *et al.*, 2004]. In the northern hemisphere, ClNO₂ mixing ratios ranging from several tens to several hundred parts per trillion (ppt) have been detected in both polluted coastal and continental regions [e.g., Osthoff *et al.*, 2008; Phillips *et al.*, 2012]. The branching ratio (or yield) of ClNO₂ (ϕ_{ClNO_2}) from H12 (Table 5) is determined by competition between N₂O₅ hydrolysis (to give HNO₃) and its reaction with aerosol Cl⁻.

Table 5. Summary of Heterogeneous Reactions Used to Model the Dechlorination of Sea-Salt Aerosol in TOMCAT and Their Reactive Uptake Coefficient (γ)

Number	Reaction	Uptake Coefficient (γ) ^a
H1	ClONO ₂ → Cl ₂	0.02
H2	ClNO ₂ → Cl ₂	0.02
H3	HOCl → Cl ₂	0.1
H4	IONO ₂ → 0.5Cl + 0.25I ₂	0.01
H5	INO ₂ → 0.5Cl + 0.25I ₂	0.02
H6	HOI → 0.5Cl + 0.25I ₂	0.06
H7	BrONO ₂ → 0.35BrCl + 0.325Br ₂	0.08
H8	BrNO ₂ → 0.35BrCl + 0.325Br ₂	0.04
H9	HOBr → 0.35BrCl + 0.325Br ₂	0.1
H10	HNO ₃ → HCl	0.5
H11	OH → 0.5Cl ₂	0.24
H12	N ₂ O ₅ → ϕ ClNO ₂ + (2- ϕ)HNO ₃	0.03 ^b

^aH1–H9: values from CAM-Chem model [Saiz-Lopez *et al.*, 2014; Fernandez *et al.*, 2014]. Originally from THAMO 1-D model [Saiz-Lopez *et al.*, 2008]. H10: reported γ of 0.5 (± 0.2) for deliquesced NaCl [Guimbaud *et al.*, 2002; Stemmler *et al.*, 2008]. H11: γ of 0.24 from model study of von Glasow [2006].

^b $\gamma = 0.005$ (RH < 60%) or $\gamma = 0.03$ (RH > 60%). Based on Evans and Jacob [2005].

Table 6. Summary of Model Experiments and the Tropospheric Chlorine Source Considered in Each

Experiment	CH ₃ Cl	VSLs	Heterogeneous Cl ^a	φ _{CINO₂}	Primary HCl Emissions ^b	Chlorocarbon Oxidation Scheme ^c
ORG1	Yes	No	No	-	No	Full
ORG2	Yes	Yes	No	-	No	Full
HET1	Yes	Yes	Yes, SS	0.50	Yes	Full
HET2	Yes	Yes	Yes, SS	0.75	Yes	Full
FULL1	Yes	Yes	Yes, SS + SUL	0.50	Yes	Full
FULL2	Yes	Yes	Yes, SS + SUL	0.75	Yes	Full
ORG2 _{Sim}	Yes	Yes	No	-	No	Simple
FULL1 _{Sim}	Yes	Yes	Yes, SS + SUL	0.50	Yes	Simple

^aSS: sea-salt dechlorination via heterogeneous reactions in Table 5. SUL: HCl recycling on sulfate aerosol (see main text).

^bHCl emissions from industry and biomass burning.

^cChlorocarbon oxidation scheme. Full: considering organic intermediates. Simple: instantaneous production of Cl atoms.

Here fixed values of φ_{CINO₂} were used, and we tested the sensitivity of our results to the assumed value (see section 2.3).

CINO₂ production is also thought to occur on non-SS surfaces, where the Cl⁻ is supplied through condensation of gas-phase HCl [e.g., *Osthoff et al.*, 2008]. Therefore, an effective reaction producing CINO₂ on SUL is necessary (R6). A simple parameterized scheme following *Yang et al.* [2010] was employed, whereby the heterogeneous reaction rate is dependent on the concentration of the locally limiting reactant and is set to the slower of the two half reactions (N₂O₅ + aerosol or HCl + aerosol). This approach assumes no chlorine accumulation on SUL and that the reaction occurs instantaneously on the substrate. In principle, the approach is also valid for several other reactions that may recycle Cl_y on SUL. Therefore, the reactions R7 to R10 were treated in a similar manner. We assumed γ values of 0.1, 0.3, 0.2, 0.2, and 0.2, for uptake of HCl, CINO₂, BrONO₂, HOCl, and HOBr on SUL, respectively.



2.3. Simulations

We performed a series of model experiments (Table 6) designed to (i) assess the relative contribution of organic versus inorganic sources to tropospheric Cl_y, (ii) examine the sensitivity of our results to the complexity of the chlorocarbon degradation scheme, and (iii) explore the relative importance of heterogeneous reactions involving chlorine on sulfate aerosol. ORG1 considered CH₃Cl only. ORG2 was identical to ORG1 but also considered the natural and anthropogenic chlorinated VSLs (summarized in Table 3). In addition to chlorocarbons, simulations HET1 and HET2 considered sea-salt dechlorination through the reactions given in Table 5, and we included industrial and biomass burning HCl emissions. In these two experiments, φ_{CINO₂} was assigned values of 0.5 and 0.75, respectively. The simulations FULL1 and FULL2 were identical to HET1 and HET2, respectively, but also included Cl_y recycling on sulfate (e.g., R6–10). The full chlorocarbon oxidation scheme (Table 4) was used in each of the above simulations.

Given mechanistic and parametric uncertainties in the fate of organic chlorinated product gases, two further sensitivity experiments were performed. These were identical to experiments ORG2 and FULL1 described above but with a simple treatment of the breakdown of chlorocarbons. Rather than using the full comprehensive oxidation scheme (Table 4), these runs assumed instantaneous release of all Cl atoms following the oxidation of CH₃Cl and VSLs (i.e., the reaction is assumed to proceed in a single step, e.g., CH₃Cl + OH → Cl and CH₂Cl₂ + OH → 2Cl), thereby neglecting chlorinated organic product gases (i.e., CCl₂O and CHClO). These experiments are labeled with the suffix “Sim.” All simulations included bromine and iodine chemistry. After

allowing the model to spin-up for 5 years (2000–2005), each simulation ran for a further 3 year period. We analyzed and present results from the year 2008. Note that the analyzed simulation year used 2008 meteorology and the anthropogenic emissions of CH_4 , CO , NO_x , etc. are also appropriate for 2008 (see section 2.1.1). However, the chemical boundary conditions of some halogenated compounds were based on 2014 surface observations (Table 3). For this reason, our analysis is not meant to be wholly representative of a specific year but is broadly appropriate for recent atmospheric conditions.

3. Results and Discussion

Sections 3.1 and 3.2 examine the chlorocarbons as a tropospheric Cl_y source. Section 3.3 evaluates the modeled HCl against observations. Section 3.4 quantifies the MBL [Cl] and examines the Cl atom precursors. The impact of Cl atoms on tropospheric CH_4 oxidation is discussed in section 3.5. Note that throughout this study we employ a *chemical tropopause* definition, with the stratosphere defined as the region above an O_3 threshold of 150 ppb.

3.1. Distribution of Chlorinated Organic Compounds

We first consider the tropospheric distribution of chlorocarbon source gases and intermediate product gases. Latitude-altitude cross sections of simulated CH_3Cl and VSLS are shown in Figure 1. Owing to its relatively long lifetime of around 1 year [Carpenter *et al.*, 2014], CH_3Cl is well mixed in the troposphere. The largest CH_3Cl mixing ratios, specified from observed surface data, occur in the tropical ($\pm 20^\circ$) boundary layer (~ 525 – 570 ppt), where vertical profile gradients, between the surface and tropopause (~ 17 km), are up to $\sim 10\%$. Given their comparatively far shorter tropospheric lifetimes (typically several months), the tropospheric distributions of VSLS exhibit larger inhomogeneity and a clear difference in the distribution of anthropogenic and naturally emitted VSLS is apparent. Owing to industrial sources, the largest mixing ratios of anthropogenic VSLS (e.g., C_2Cl_4 and $\text{CH}_2\text{ClCH}_2\text{Cl}$) occur in the northern hemisphere (NH), and hemispheric gradients are pronounced. Surface mixing ratios of CH_2Cl_2 , the most abundant (anthropogenic) chlorinated VSLS, are >60 ppt in the NH. This is far larger than the global mean surface mixing ratios assumed in recent modeling work [Schmidt *et al.*, 2016], which seem inconsistent with the most recent surface observations of CH_2Cl_2 . In contrast, the largest mixing ratios of the oceanic chlorocarbons (Figures 1g–1i) occur in the tropics.

Recall from section 2.2.1 that for CH_3Cl , CH_2Cl_2 , CHCl_3 , and C_2Cl_4 , the model uses a latitude-dependent surface boundary condition based on NOAA and AGAGE measurements. Compared to independent observations of these compounds, from the HIPPO aircraft mission [Wofsy *et al.*, 2011, 2016], the model captures hemispheric gradients well and absolute values are generally in close agreement (Figure 2). Note that for CH_2Cl_2 the apparent high model bias in the NH (Figure 2a) is to be expected as our prescribed surface boundary condition is appropriate for 2014. The HIPPO data were obtained between 2009 and 2011, and CH_2Cl_2 has increased significantly in this intervening period [Hossaini *et al.*, 2015a, 2015b].

The total organic chlorine contained in source gases (Figure 3) is greatest between 30 and 60°N, where it approaches around 800 ppt Cl at the surface (here, VSLS account for around $\sim 25\%$ of this total). The VSLS contribution exhibits a strong hemispheric asymmetry as shown in Figure 3b. On this basis, it seems appropriate that global models that impose surface mixing ratio boundary conditions for VSLS consider latitudinal gradients (i.e., do not assume a single and uniform global mean value at the surface). Vertical gradients (i.e., amount lost) in total organic chlorine from VSLS, between the surface and tropical tropopause, are up to $\sim 30\%$. The breakdown of VSLS (and CH_3Cl) produces a range of chlorinated organic products. CCl_2O and CHClO are the most abundant organic products, with simulated tropospheric mixing ratios of all others <1 ppt. Latitude-altitude cross sections of CCl_2O , CHClO , and total organic chlorine in product gases (reasonably approximated as $2 \times \text{CCl}_2\text{O} + \text{CHClO}$) are shown in Figure 4. Previous studies have considered CCl_2O and CHClO as potential carriers of chlorine to the stratosphere [e.g., Wild *et al.*, 1996; Hossaini *et al.*, 2015b]. CCl_2O is an oxidation product of CHCl_3 and C_2Cl_4 . It is only sparingly soluble in water but is very rapidly hydrolyzed once in solution [e.g., Kindler *et al.*, 1995]. The latter effect, which can occur in cloud, was not considered here, and thus, modeled tropospheric CCl_2O mixing ratios shown in Figure 4 are likely to be upper limits.

As far as we know, no atmospheric observations of CHClO exist. The largest simulated CHClO mixing ratios (~ 15 ppt) are in the NH, where its main precursor (CH_2Cl_2) is most abundant. Recent MCM modeling has

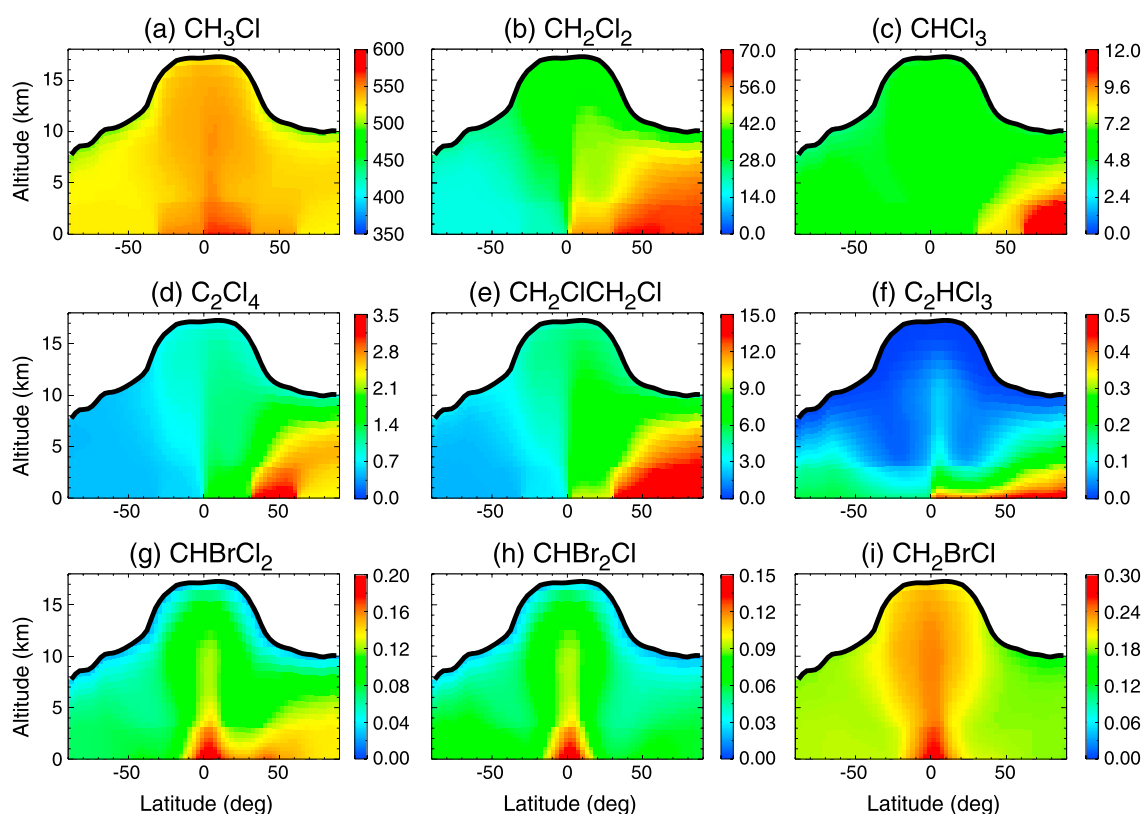


Figure 1. Annual and zonal mean latitude-altitude cross sections of (a) CH_3Cl , (b) CH_2Cl_2 , (c) CHCl_3 , (d) C_2Cl_4 , (e) $\text{CH}_2\text{ClCH}_2\text{Cl}$, (f) C_2HCl_3 , (g) CHBrCl_2 , (h) CHBr_2Cl , and (i) CH_2BrCl volume mixing ratio (ppt) in the troposphere. Note the differing color scales. The location of the tropopause (150 ppb O_3) is marked by a thick black line. Model output from experiment ORG2.

shown that CHClO may also be produced following the addition of Cl atoms to alkenes (not considered here) [Riedel *et al.*, 2014]. To our knowledge, the same study did not consider CH_2Cl_2 oxidation as a CHClO source but concluded that CHClO photolysis could provide an atomic Cl source comparable to that of HOCl photolysis. We calculate partial tropospheric mean CHClO lifetimes of 32, 372, and 865 days against reactions with OH and NO_3 and due to photolysis, respectively. The partial lifetime against oxidation with Cl was >20 years. Our overall tropospheric CHClO lifetime with respect to these processes (~ 1 month) is similar to the estimate of 26 days reported by Libuda *et al.* [1990]. It has also been suggested that CHClO may be lost via uptake to aerosol, with reactions on sea salt potentially producing HCl [Toyota *et al.*, 2004]. Given the uncertainty in such a process and a lack of information in the literature, we did not consider it here. Besides, by performing simulations using both the comprehensive and simple chlorocarbon oxidation schemes, uncertainties in the atmospheric fate of organic product gases, such as CHClO , are captured in our ensemble of experiments.

3.2. Inorganic Chlorine Derived From Chlorocarbons

While sea-salt dechlorination is likely the largest source of tropospheric Cl_y [e.g., Graedel and Keene, 1995], chlorocarbon oxidation provides an additional contribution. This contribution from chlorocarbons is poorly quantified in the present day as (i) previous assessments have not considered all VSLs present in the atmosphere and (ii) the concentrations of several anthropogenic VSLs have changed substantially in recent years. Based on simulations using the full chlorocarbon oxidation scheme, CH_3Cl oxidation (ORG1) maintains a small (<5 ppt) background level of Cl_y ($\text{HCl} + \text{HOCl} + \text{ClONO}_2 + \text{ClONO}_2 + 2 \times \text{Cl}_2 + \text{OCIO} + \text{BrCl} + \text{ICl}$) throughout most of the free troposphere, with larger levels present in the upper troposphere (Figure 5a). When VSL oxidation is also considered (ORG2), around 8–12 ppt of Cl_y is present in large areas of the free troposphere (i.e., Figure 5b). Larger Cl_y mixing ratios of >20 ppt in the free troposphere are predicted from ORG2_{sim} (Figure 5c). The sensitivity of simulated Cl_y from CH_3Cl + VSLs to the chlorocarbon oxidation scheme is greatest in the NH, where

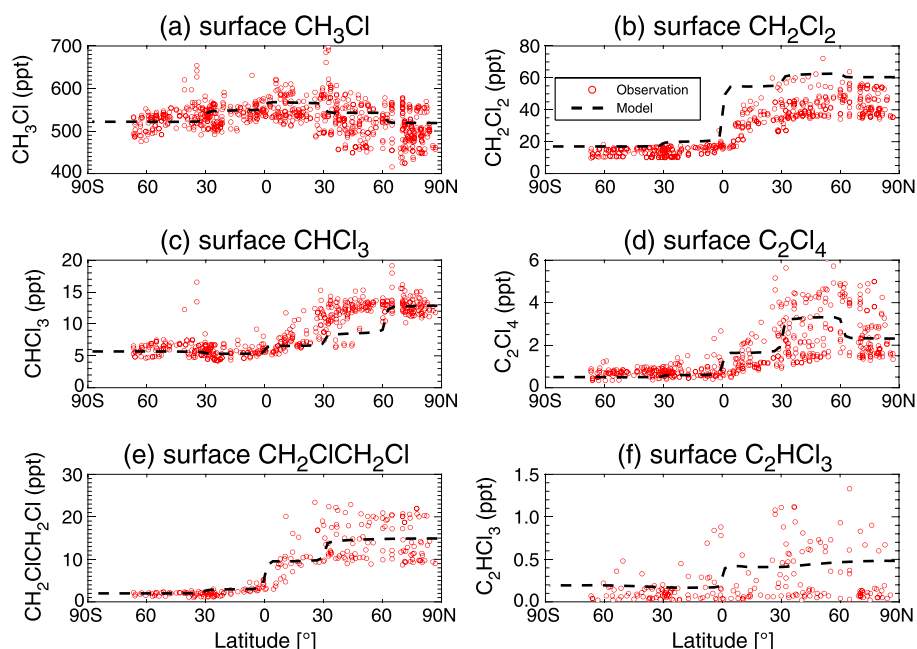


Figure 2. Observed boundary layer surface volume mixing ratio (ppt) of (a) CH_3Cl , (b) CH_2Cl_2 , (c) CHCl_3 , (d) C_2Cl_4 , (e) $\text{CH}_2\text{ClCH}_2\text{Cl}$, and (f) C_2HCl_3 as a function of latitude. Observed values (circles) are a compilation of measurements obtained during the 2009–2011 NSF HIPPO campaign [Wofsy *et al.*, 2011]. Also shown is the imposed surface mixing ratio boundary condition in TOMCAT (dashed line; see main text).

anthropogenic VSLs are most prevalent. Tropospheric Cl_y in simulation ORG2_{sim} is up to ~ 10 ppt larger than that from ORG2 as shown in Figure 5d. The contribution of chlorocarbon oxidation to the *total* modeled Cl_y field (i.e., including inorganic chlorine sources) is variable depending on location. Figure S1 in the supporting information shows that the initial oxidation of chlorocarbons can account for between near zero and $\sim 10\%$ of total

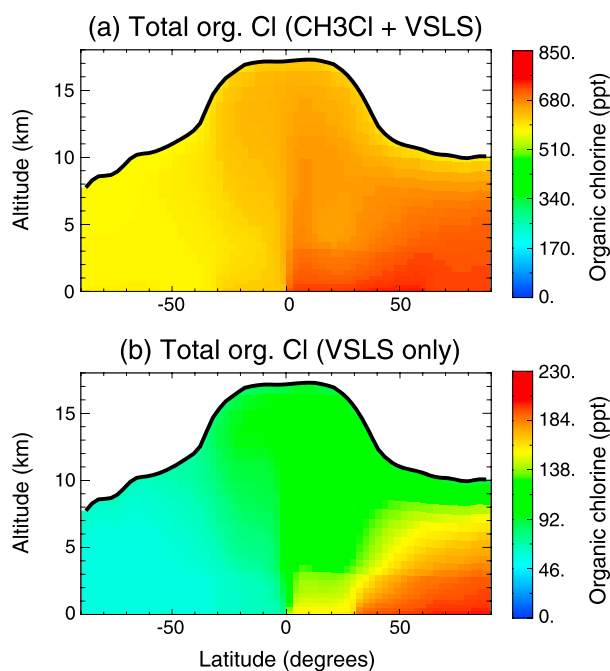


Figure 3. Annual and zonal mean latitude-altitude cross sections of total organic chlorine (ppt Cl) in sources gases for (a) CH_3Cl + VSLs and (b) VSLs only. Model data for Figure 3a are from experiment ORG2 , while for Figure 3b the data are calculated from $\text{ORG2} - \text{ORG1}$.

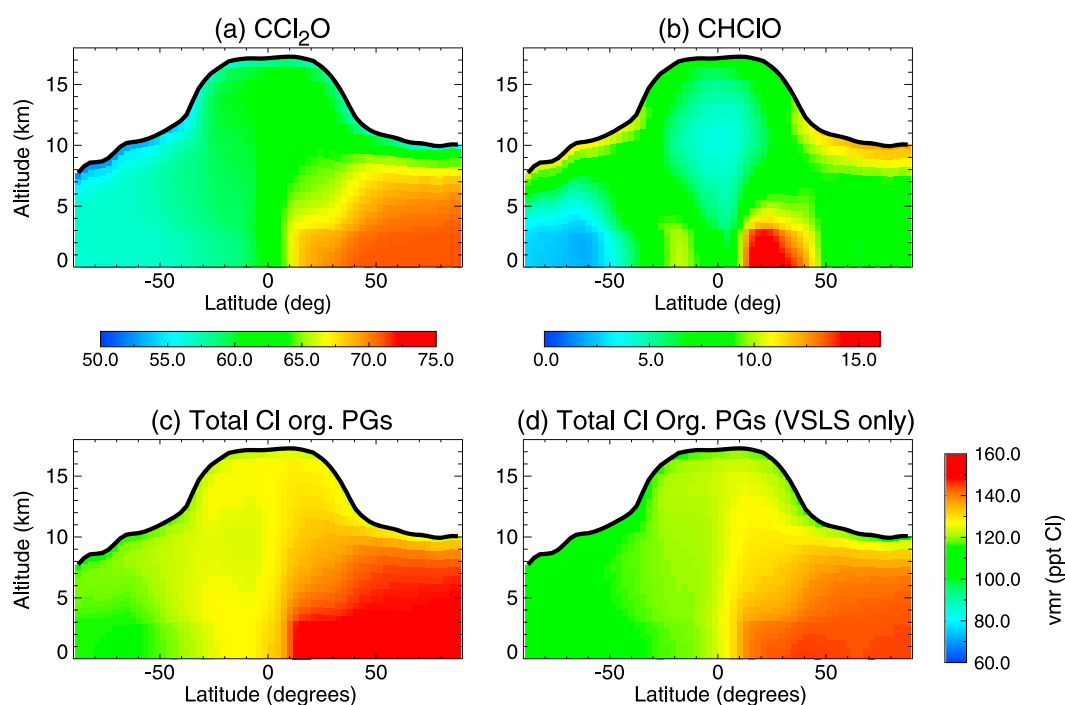


Figure 4. Annual and zonal mean latitude-altitude cross sections of (a) CCl_2O and (b) CHClO volume mixing ratio (ppt) in the troposphere. (c) Total chlorine (ppt Cl) in organic product gases (defined as $2 \times \text{CCl}_2\text{O} + \text{CHClO} +$ other minor organic products; see main text). (d) Equivalent to Figure 4c but shows summed chlorine in organic products arising from VLSL oxidation only (i.e., excluding contributions derived from CH_3Cl). Model data for Figures 4a–4c are from experiment ORG2, while for Figure 4d the data are calculated from ORG2 – ORG1.

Cl_y in the boundary layer, between 20 and 30% in the free troposphere, and up to ~50% in the upper troposphere—reflecting a diminishing influence of the chlorine source from sea salt and industry/biomass burning, with altitude. Note that we considered CH_3Cl and chlorinated VLSL only. The stratosphere-to-troposphere exchange of Cl-rich air (from the breakdown of CFCs, HCFCs, and other gases) would mean that the actual relative contribution of *all* chlorocarbons present in the atmosphere to upper tropospheric Cl_y would likely be greater. In addition, we note that in the ORG simulations, in which sea-salt chlorine is not included, the lifetimes of CH_3Cl and VLSL against Cl atom oxidation in the troposphere (particularly in the MBL) are likely overestimated. However, as loss of these compounds occurs predominately through OH oxidation, this effect is expected to be fairly minor.

Previous assessments of tropospheric Cl_y have not considered organic intermediates in the oxidation chain of chlorocarbons. In terms of Cl_y production from chlorocarbon oxidation, an appropriate comparison to those studies can therefore be made from experiment ORG2_{sim}. Of the chlorocarbons considered, CH_3Cl oxidation provides the largest Cl_y source of 2299 Gg Cl/yr—within ~10% of the previous estimates (Table 7). The summed Cl_y source from all VLSL (2023 Gg Cl/yr) is comparable to that from CH_3Cl , with the anthropogenic VLSL, CH_2Cl_2 , making the single largest contribution (1044 Gg Cl/yr). Tropospheric levels of CH_2Cl_2 have doubled in the last decade [Hossaini et al., 2015a, 2015b]. Our estimate of Cl_y production from CH_2Cl_2 is, therefore, a factor of ~2 greater than that of previous assessments [Keene et al., 1999; Schmidt et al., 2016] that were either unable to or did not account for this growth. Our results for C_2Cl_4 (106 Gg Cl/yr) and C_2HCl_3 (150 Gg Cl/yr) are significantly lower than those of Keene et al. [1999], as levels of these anthropogenic VLSL have declined in recent years [e.g., Simmonds et al., 2006; Hossaini et al., 2015b]. Compared to anthropogenic VLSL, naturally emitted CHBrCl_2 , CHBr_2Cl , and CH_2BrCl are minor tropospheric Cl_y sources, providing around 12 Gg Cl/yr in total.

We find that the total tropospheric Cl_y production from chlorocarbons is sensitive to the choice of chlorocarbon oxidation scheme. Cl_y production in ORG2_{sim} (4322 Gg Cl/yr) is around a factor of 3 larger than that from ORG2 (1403 Gg Cl/yr). This is because, as previously noted, a number of chlorinated organic products

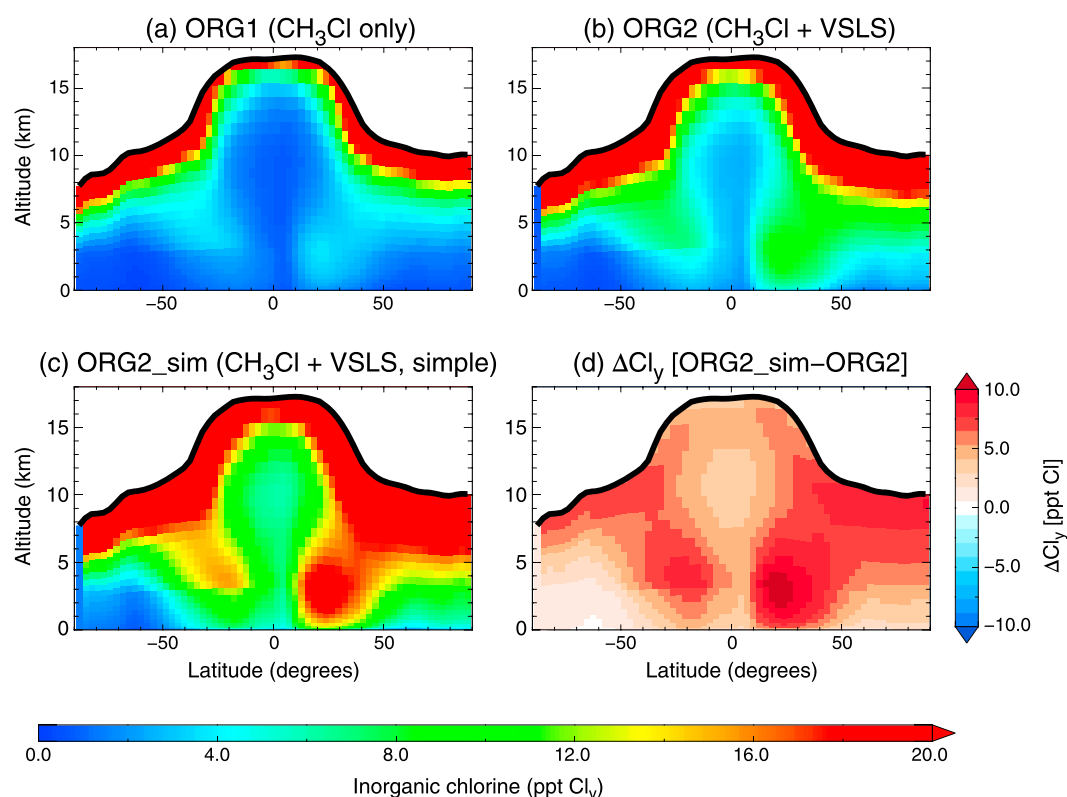


Figure 5. Annual and zonal mean latitude-altitude cross sections of inorganic chlorine (Cl_y ; ppt) derived from (a) CH_3Cl (ORG1), (b) CH_3Cl + VSLs (ORG2), and (c) CH_3Cl + VSLs (ORG2_{sim}, i.e., simple organic oxidation scheme). (d) The Cl_y difference (ORG2_{sim} – ORG2) and therefore the difference arising from use of the simple and full chlorocarbon oxidation schemes.

(produced in ORG2 but not ORG2_{sim}) are subject to deposition processes and CCl_2O , a major product of several chlorocarbon source gases (such as $CHCl_3$), is long-lived (e.g. CCl_2O can be transported to the stratosphere and release Cl_y as part of the stratospheric budget). Therefore, the assumption of instantaneous release of Cl atoms from chlorocarbons, as in recent model studies [e.g., Ordóñez *et al.*, 2012; Sherwen *et al.*, 2016], will likely lead to an overestimation of tropospheric Cl_y . However, we acknowledge that there are clearly both mechanistic and kinetic uncertainties related to the chlorocarbon oxidation chain, and note that we did not include possible heterogeneous/multi-phase processing of $CHClO$ and CCl_2O . The significance of these findings for MBL [Cl] and CH_4 oxidation is later discussed. Note that in principle Cl_y released from chlorocarbons could, in the MBL, activate further chlorine from sea salt (i.e., due to the reactions in Table 5). However, as the objective here is to quantify Cl_y production solely from chlorocarbon oxidation, the above analysis and values from ORG2_{sim} in Table 7 are based on the loss rate of the chlorocarbons only and do not include such an effect.

Table 7. Global Tropospheric Source of Cl_y (Gg Cl/yr) From Chlorocarbon Oxidation

Source	This Work (ORG2)	This Work (ORG2 _{sim})	Keene <i>et al.</i> [1999]	Sherwen <i>et al.</i> [2016]
CH_3Cl	-	2299	2400	2100
CH_2Cl_2	-	1044	490	570
$CHCl_3$	-	232	410	250
C_2Cl_4	-	106	440	-
C_2HCl_3	-	150	350	-
CH_2ClCH_2Cl	-	386	-	-
$CHBrCl_2$	-	6	-	-
$CHBr_2Cl$	-	3	-	-
CH_2BrCl	-	3	-	-
CH_2I_2	-	93	-	-
Total Cl_y production	1403	4322	4090	2920

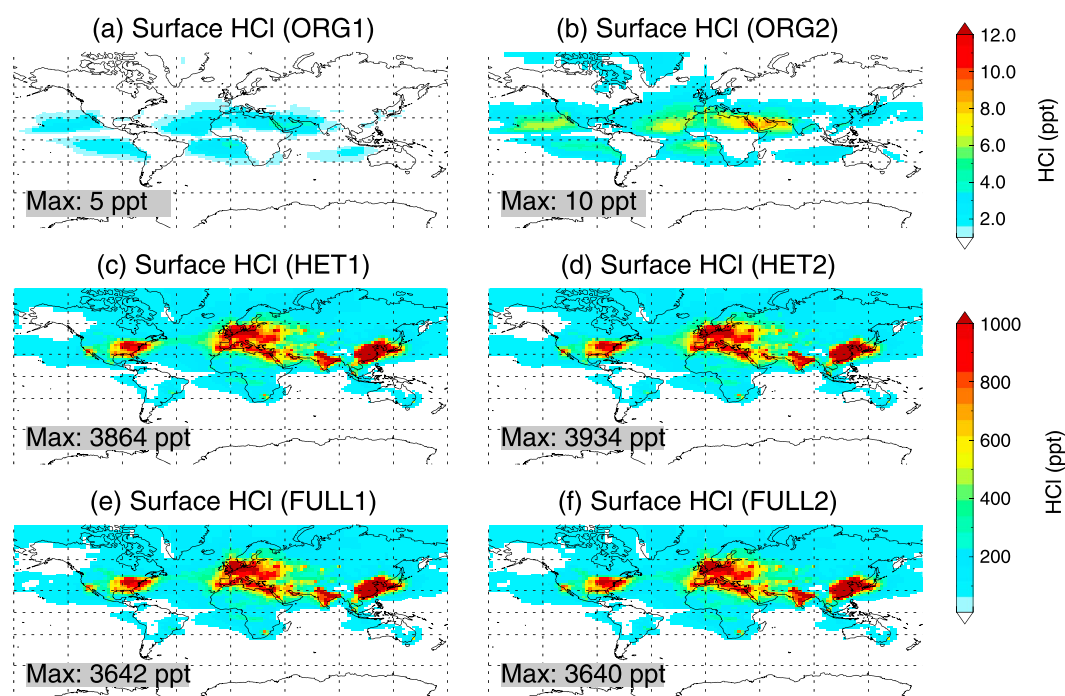


Figure 6. Annual mean surface volume mixing ratio (ppt) of HCl from (a) ORG1 (CH_3Cl only), (b) ORG2 (CH_3Cl + VSLS), (c) HET1 (organic + inorganic Cl sources; $\phi_{\text{ClNO}_2} = 0.5$), (d) HET2 (as HET1 but $\phi_{\text{ClNO}_2} = 0.75$), (e) FULL1 (as HET1 with HCl recycling on sulfate), and (f) FULL2 (as HET2 with HCl recycling on sulfate). Maximum values are annotated. Note the change in scale from Figures 6a and 6b to 6c–6f.

3.3. Boundary Layer HCl

Most Cl_y in the troposphere resides as HCl, which is directly emitted from combustion processes [e.g., McCulloch *et al.*, 1999], released from sea-salt aerosol through acid displacement (e.g., Table 5, H10), and produced following the reaction of atomic Cl with VOCs (e.g., Table 1). However, measurements of HCl throughout the global troposphere are generally sparse. Most HCl measurements have been obtained in polluted coastal or continental regions at the surface, where HCl mixing ratios can exhibit extremely large variability and often exceed several parts per billion [e.g., Bari *et al.*, 2003; Keene *et al.*, 2007; Crisp *et al.*, 2014]. At remote and semi-remote sites, HCl levels are generally lower and of the order of several tens to several hundred parts per trillion [e.g., Sanhueza and Garaboto, 2002; Sander *et al.*, 2013].

Figure 6 shows the simulated annual mean surface distribution of HCl. Considering CH_3Cl and VSLS only (i.e., ORG2), annual mean surface HCl is <10 ppt in most regions. As expected, far greater HCl mixing ratios are generated when inorganic sources (i.e., sea-salt dechlorination and industry/biomass burning emissions) are also considered. Recall from section 3.2 that chlorocarbon oxidation provides a source of up to ~4320 Gg Cl/yr in TOMCAT. For comparison, the sea-salt dechlorination reactions in Table 5, excluding acid displacement of HCl by HNO_3 (see discussion below), provide a source of ~5550 Gg Cl/yr. This order of magnitude seems reasonable when compared to the recent estimate of 6050 Gg Cl/yr reported in the modeling study of Schmidt *et al.* [2016]. Our model predicts the largest HCl mixing ratios (up to several parts per billion) over continental regions, particularly over Europe, the East Coast of the U.S., and over both central and East Asia. Elevated levels of HCl over these polluted regions are due to acid displacement of HCl from sea-salt aerosol, following uptake of HNO_3 (reaction H10 in Table 5), as also shown in several measurement- [e.g., Keene *et al.*, 2007] and model-based [e.g., Pechtl and von Glasow, 2007] studies. In addition, primary HCl emissions from combustion are greatest in these regions [McCulloch *et al.*, 1999]. Note that reaction H10 in Table 5 provides a source of ~90 Tg Cl/yr in TOMCAT. This is a larger source than the range of ~37–73 Tg Cl/yr due to HCl acid displacement estimated by Graedel and Keene [1995], possibly due to the different time period over which our study examines. However, we note that TOMCAT reproduces MBL HCl measurements at various locations well (see below). We find that larger maximum HCl levels are generated in experiment HET2 compared to HET1, owing to the larger ClNO_2 yield in the former.

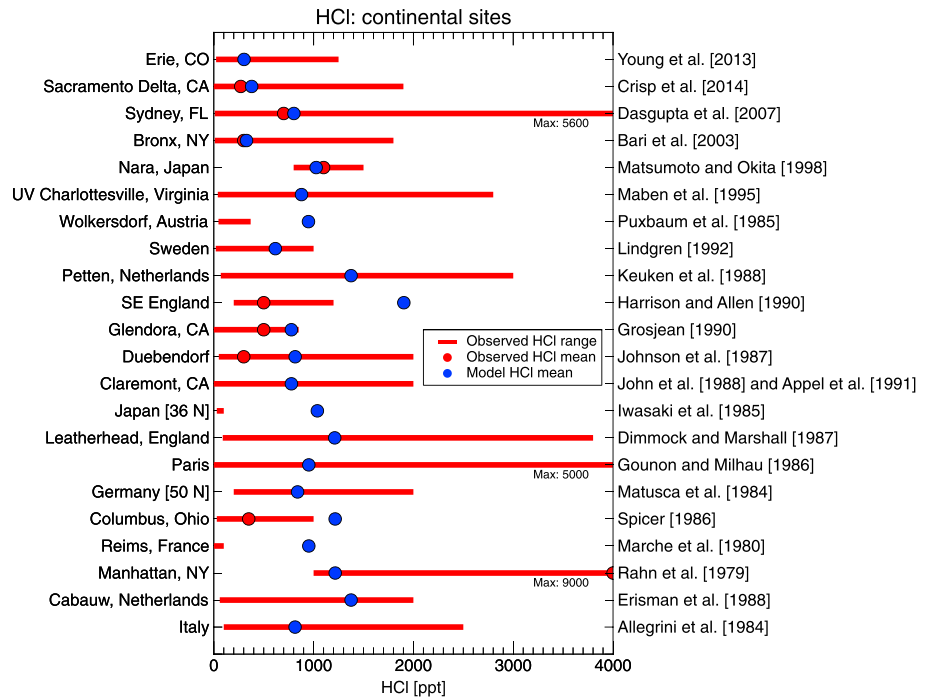


Figure 7. Comparison of modeled annual mean surface HCl (ppt) at continental locations with observed values. In some sites, a mean value was not reported and just the range is given. Model output from experiment HET2. Measurement data: Young et al. [2013], Crisp et al. [2014], Dasgupta et al. [2007], Bari et al. [2003], Matsumoto and Okita [1998], Maben et al. [1995], Puxbaum et al. [1985], Lindgren et al. [1992], Keuken et al. [1988], Harrison and Allen [1990], Grosjean [1990], Johnson et al. [1987], John et al. [1988] and Appel et al. [1991], Iwasaki et al. [1985], Dimmock and Marshall [1987], Gounon and Milhau [1986], Matusca et al. [1984], Spicer [1986], Marché et al. [1980], Rahn et al. [1979], Erisman et al. [1988] and Allegrini et al. [1984].

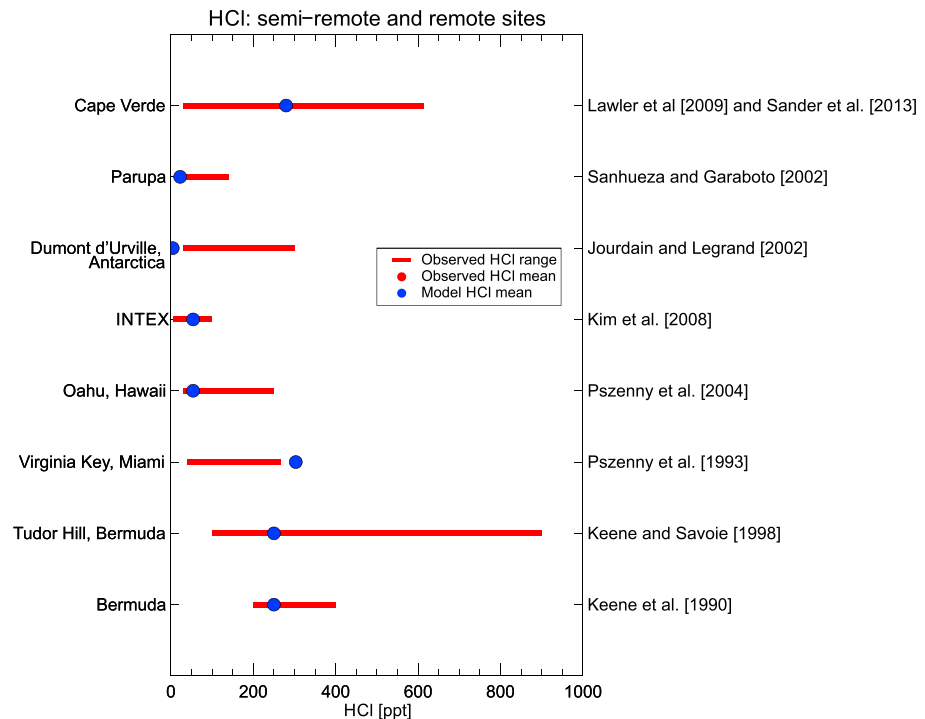


Figure 8. Same as in Figure 7 but for remote and semi-remote locations. Measurement data: Lawler et al. [2009], Sander et al. [2003], Sanhueza and Garaboto [2002], Jourdain and Legrand [2002], Kim et al. [2008], Pszeny et al. [1993, 2004], Keene and Savoie [1998] and Keene et al. [1990].

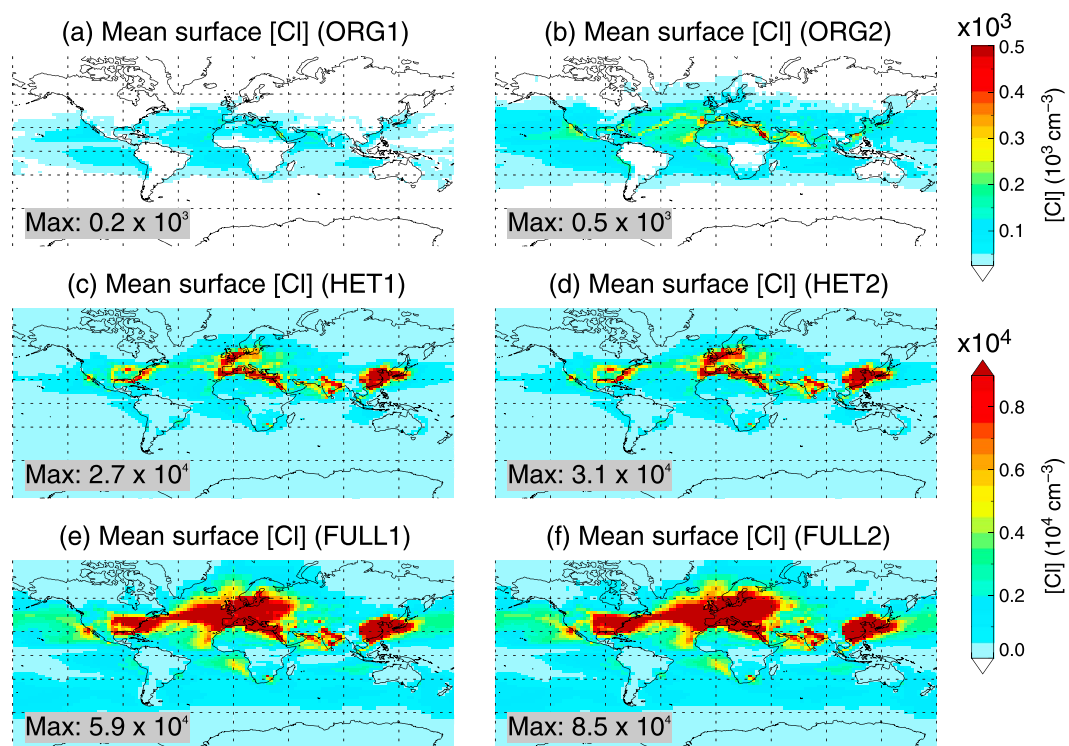


Figure 9. Annual mean surface [Cl] (atoms cm^{-3}) from (a) ORG1, (b) ORG2, (c) HET1, (d) HET2, (e) FULL1, and (f) FULL2. Maximum values are annotated. Note the difference in scales between Figures 9a and 9b and 9c–9f.

A comparison of model surface HCl to measurements obtained in continental and remote/semi-remote locations is given in Figures 7 and 8, respectively. The observed data are based on a recent HCl measurement compilation [Crisp *et al.*, 2014]. These comparisons reveal that the simulated abundance of HCl is generally realistic. At the majority of sites, modeled HCl falls within the measured range and TOMCAT generally captures the spatial variability of HCl, with greatly elevated levels in polluted continental regions and far lower values in remote/semiremote regions (e.g., Cape Verde). Based on HCl measured in Antarctica [Jourdain and Legrand, 2002], the model may underestimate chlorine production at high latitudes in the southern hemisphere. However, broadly, the spatial HCl distribution and hemispheric asymmetry are in agreement with the model study of Erickson *et al.* [1999], which also reported the largest HCl production in the NH, especially in the North Atlantic and in regions downwind of Asian sources of acidic gases.

3.4. Chlorine Atoms and Photolabile Precursors

Figure 9 shows the simulated annual mean surface [Cl]. We find that CH_3Cl oxidation provides a small [Cl] background of around $0.5\text{--}2 \times 10^2 \text{ atoms cm}^{-3}$ throughout most of the global boundary layer. When VSLs are also considered (i.e., ORG2), annual mean [Cl] reaches a maximum of $0.5 \times 10^3 \text{ atoms cm}^{-3}$ in some coastal regions of the NH. Note that the local lifetime of VSLs exhibits significant seasonal variability and surface [Cl] in ORG2 exceeds $1 \times 10^3 \text{ atoms cm}^{-3}$ in some locations during summer months (not shown). Similarly, many Cl precursors (e.g., Cl_2 and BrCl) are readily photolyzed; thus, [Cl] exhibits a marked diurnal cycle. Daytime [Cl] is larger than the annual averages shown in Figure 9 (see modeled midday [Cl] in Figure S2).

As expected, the largest [Cl] levels (note the scale change) are generated when inorganic chlorine sources are also considered. In all HET and FULL experiments, [Cl] is $>1 \times 10^4 \text{ atoms cm}^{-3}$ over large coastal/continental regions of the polluted NH (and exceeds $10^5 \text{ atoms cm}^{-3}$ in some regions at midday; Figure S2). As discussed in section 3.3, HCl is abundant in these regions due to the combined influence of acid displacement from sea salt (owing to elevated HNO_3) and due to primary HCl emissions. Where HCl is abundant, oxidation of HCl sustains the relatively large [Cl] levels, and further release of Cl_y from aerosol—an autocatalytic process—is initiated. Other factors contribute to elevated [Cl] in the polluted NH, including the production of ClNO_2 (see later discussion), and the recycling of HCl on sulfate aerosol. The effect of the latter can be seen by

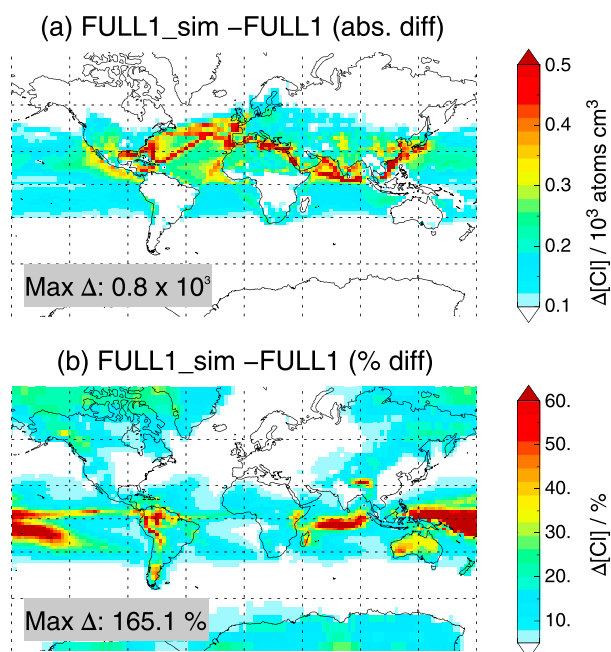


Figure 10. Difference in surface [Cl] between runs FULL1_{sim} and FULL1 in (a) absolute (10^3 atoms cm^{-3}) and (b) percentage (%) terms.

comparing Figures 9c and 9d with 9e and 9f. Maximum [Cl] levels are larger, reaching $>5 \times 10^4$ atoms cm^{-3} , when HCl recycling on sulfate aerosol is considered, compared to simulations considering heterogeneous chlorine chemistry on sea-salt aerosol only. Several previous studies have reported [Cl] of this order in polluted coastal air [e.g., Keene *et al.*, 2007]. Overall, the link demonstrated in our global model between anthropogenic pollution sources and active chlorine chemistry is consistent with the same notion previously established by several measurement- and 1-D model-based studies [e.g., Pechtl and von Glasow, 2007; Lawler *et al.*, 2009, 2011]. Accordingly, our results indicate a strong hemispheric gradient in [Cl]. Some of the lowest [Cl] levels are predicted over the Southern Ocean (assumed 60°S – 80°S), where modeled surface [Cl] ranges from near zero to around 1×10^3 atoms cm^{-3} .

Broadly, this is in agreement with Wingenter *et al.* [1999], who inferred [Cl] levels of around of 720 (± 100) atoms cm^{-3} in this region. Overall, [Cl] levels in TOMCAT seem realistic and fall within the large range of previous measurement-based estimates, 10^3 to 10^5 atoms cm^{-3} [Saiz-Lopez and von Glasow, 2012, and references therein]. The air mass-weighted tropospheric mean [Cl] is 1.3×10^3 atoms cm^{-3} from simulation FULL1.

We also examined the sensitivity of surface [Cl] to the choice of chlorocarbon oxidation scheme. Figure 10 compares the annual mean surface [Cl] from FULL1 and FULL1_{sim}, in absolute and percent terms. The simple oxidation scheme yields larger [Cl] levels, with typical differences of 0.1 – 0.2×10^3 atoms cm^{-3} in the tropical MBL (where the lifetime of VLS is shortest) and $>0.5 \times 10^3$ atoms cm^{-3} in some coastal regions. Regionally, such differences would appear to be quite significant, given that a lower limit of MBL [Cl] is generally regarded as on the order of 10^3 atoms cm^{-3} [Saiz-Lopez and von Glasow, 2012]. In percent terms, [Cl] in FULL1_{sim} is $\sim 10\%$ to $>100\%$ larger, depending on region. The assumptions made regarding chlorocarbon oxidation in models, therefore, need to be considered when evaluating uncertainty in model-derived [Cl] estimates and intermodel differences.

Observations of (non-HCl) Cl atom precursors are generally sparse, although in recent years CINO₂ detection has been a major focus of a number of campaigns. CINO₂ mixing ratios of typically several hundred parts per trillion have been observed in coastal [e.g., Osthoff *et al.*, 2008; Riedel *et al.*, 2012] and continental regions [e.g., Thornton *et al.*, 2010; Mielke *et al.*, 2011] of the U.S. and Canada and over Europe [Phillips *et al.*, 2012; Bannan *et al.*, 2015]. These measurements highlight a strong CINO₂ diurnal cycle related to nocturnal production from N₂O₅, with maximum CINO₂ concentrations generally observed before sunrise. Figure 11 compares the modeled annual mean CINO₂ at the surface from experiments HET2 (no CINO₂ production on sulfate) and FULL2 (with CINO₂ production on sulfate). CINO₂ production in TOMCAT is limited to high NO_x regions and is largest in East Asia. Large differences between the HET2 and FULL2 simulations are apparent, with maximum CINO₂ levels in the latter up to $\sim 4\times$ greater. This highlights the importance of CINO₂ production on sulfate, following HCl condensation, and is consistent with current understanding of CINO₂ production from measurement and modeling studies [e.g., von Glasow, 2008; Thornton *et al.*, 2010; Long *et al.*, 2014]. The magnitude of surface CINO₂ in TOMCAT is similar to that of the global model study of Long *et al.* [2014]—i.e., annual mean values on the order of 80–120 ppt in the above NH regions. Figure S3 shows the modeled mean surface CINO₂ mixing ratio at 5 A.M. local time (for assumed ϕ_{CINO_2} of 0.5). Before sunrise, modeled CINO₂ mixing ratios

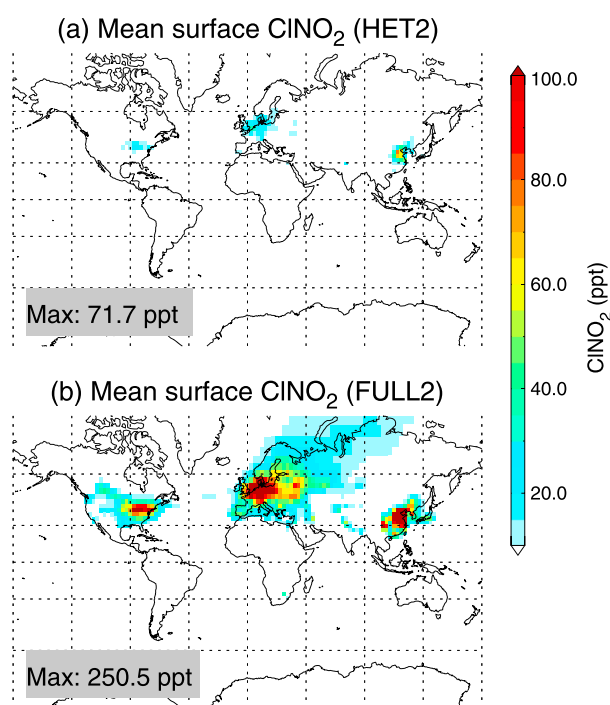


Figure 11. Annual mean ClNO_2 surface mixing ratio (ppt) from model experiments (a) HET2 and (b) FULL2.

West Coast where, for example, a mean nighttime value of 120 ppt has been reported off the Californian coast [Riedel *et al.*, 2012]. The model of Sarwar *et al.* [2012] predicted mean daily maximum ClNO_2 mixing ratios of >400 ppt in the months of February and September over Southern California. The equivalent TOMCAT values in this region rarely exceed several tens of parts per trillion, although values of ~ 60 ppt are present along the West Coast in winter (Figure S4). The reason for this apparent underestimation of ClNO_2 is unclear, but it is potentially due to a combination of (i) an underestimation of regional NO_x emissions, although at the global scale NO_x emissions in TOMCAT are reasonable [Monks *et al.*, 2016]; (ii) an underestimation of localized chlorine sources (e.g., swimming pools and power plants) and/or sea-salt/sulfate aerosol that would increase ClNO_2 production (e.g., through R6; section 2.2.2); or finally, (iii) the assumed ClNO_2 yield following N_2O_5 uptake to aerosol. On the latter point, our model assumes that $\phi_{\text{ClNO}_2} = 0.5$ or 0.75 , although values approaching 1.0 for coarse particulate matter over Coastal California have been predicted [Sarwar *et al.*, 2012]. The resolution of the global model may also be a reason for underestimating ClNO_2 hot spot regions considering the spatial variability of the above processes.

Limited measurements of Cl_2 in the MBL have also been reported. Finley and Saltzman [2006, 2008] detected ~ 2 – 26 ppt of Cl_2 in coastal air in California. Cl_2 mixing ratios >100 ppt have been observed in coastal sites experiencing polluted continental outflow [Spicer *et al.*, 1998; Lawler *et al.*, 2009]. The simulated annual mean surface mixing ratio of Cl_2 is shown in Figure S5. Cl_2 exhibits a very similar spatial pattern to that shown in Figure 11 (i.e., coincident with elevated ClNO_2), with mixing ratios less than 5 ppt over most of the globe but with levels reaching several tens of parts per trillion in polluted regions and, in a small number of model grid boxes over East Asia, up to ~ 200 ppt.

3.5. Methane Oxidation

The column-integrated CH_4 loss rate due to OH and Cl (summed over the depth of the troposphere) is shown in Figure 12 (experiment FULL1). Globally, oxidation by OH is the dominant chemical sink of CH_4 , and in TOMCAT, the chemical CH_4 lifetime with respect to tropospheric OH (τ_{OH}) is 10 years (Table 8). This is in reasonable agreement to the multimodel mean estimate of $9.3 (\pm 0.9)$ years reported by Voulgarakis *et al.* [2013], which used the same tropopause definition (i.e., 150 ppb ozone threshold), and is also consistent with the

of up to several hundred parts per trillion are typical of measured values reported in recent work [e.g., Simpson *et al.*, 2015, and references therein]. For example, Bannan *et al.* [2015] reported a mean ClNO_2 diurnal cycle over London that peaked between 4 A.M. and 5 A.M. and with mean ClNO_2 mixing ratios of ~ 150 ppt at this time. Here the modeled mean ClNO_2 mixing ratio over London at 5 A.M. is 200 ppt.

Over the U.S., TOMCAT predicts the largest surface ClNO_2 mixing ratios along the East Coast. Here the regional-focused model study of Sarwar *et al.* [2012] predicted mean daily maximum ClNO_2 mixing ratios typically in the range of ~ 240 – 480 ppt in February. The equivalent TOMCAT ClNO_2 field (mean of daily maximum in February) is shown in Figure S4. Along the East Coast of the U.S., modeled ClNO_2 exceeds 350 ppt in some regions. However, the model appears to significantly underestimate ClNO_2 over the

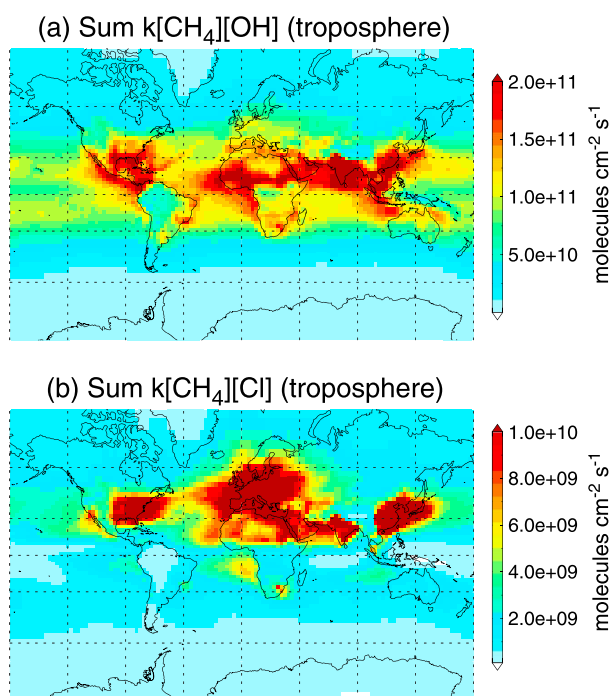


Figure 12. Annual mean tropospheric column-integrated reaction rate (molecules $\text{cm}^{-2} \text{s}^{-1}$) for (a) $\text{CH}_4 + \text{OH}$ and (b) $\text{CH}_4 + \text{Cl}$. Note the difference in scales. Model output from experiment FULL1.

recent measurement-based estimate of $11.2 (\pm 1.3)$ reported by *Prather et al.* [2012]. In percent terms, the contribution of Cl to the total CH_4 chemical sink (i.e., from both OH and Cl) in the boundary layer, and also for the entire tropospheric column, is shown in Figure 13. Cl accounts for up to several percent of total CH_4 oxidation throughout most of the boundary layer and between 10 and 20% over large areas of the polluted NH and over the Southern Ocean. In a small number of model grid boxes values up to $\sim 34\%$ occur. Previously, *Lawler et al.* [2011] estimated that Cl atoms could account for 10–15% of total CH_4 oxidation at the Cape Verde Atmospheric Observatory, based on data-constrained box model simulations. They inferred the largest percentage Cl contributions at times when the site experienced aged polluted air from mainland Europe. In the vicinity of Cape Verde, our modeled contri-

bution (around 6%) is lower on average than the estimate of *Lawler et al.* [2011], though within the range of 5.4–11.6% reported by the model study of *Sommariva and von Glasow* [2012]. We note that we would not expect to capture the specific conditions under which the measurements of *Lawler et al.* [2011] were obtained. Further, their estimate of 10–15% is compatible with our estimates in other coastal regions that experience polluted conditions. Overall, the significance of the $\text{CH}_4 + \text{Cl}$ sink is likely to vary substantially with region.

Few estimates of the global significance of the $\text{CH}_4 + \text{Cl}$ sink have been reported. *Lawler et al.* [2009] estimated that Cl could account for up to 7% of global CH_4 oxidation by extrapolating inferred levels of [Cl] at Cape Verde. This estimate assumed that [Cl] levels, derived at the site under polluted conditions, were representative of the whole tropical MBL. A smaller contribution of 2% was derived for “clean” conditions. Our results (Table 8) suggest that Cl atoms account for around 2.5–2.7% of the global total CH_4 oxidation in the troposphere and are therefore in reasonable agreement with the lower, clean case, reported by *Lawler et al.* [2009]. By examining the observed apparent kinetic isotope effect (KIE) of the CH_4 atmospheric sink, *Allan et al.* [2007] estimated a global CH_4 sink of 13–37 Tg CH_4/yr due to Cl in the troposphere. Similarly, *Platt et al.* [2004] analyzed the observed isotope effects in methane and estimated a sink of 19 Tg CH_4/yr . Our analogous estimates are around 12–13 Tg CH_4/yr and are therefore at the lower limit of those studies. In our experiments the assumed ClNO_2 yield (i.e., assumed φ_{ClNO_2} of either 0.5 or 0.75), following N_2O_5 uptake to aerosol, and details of the chlorocarbon oxidation scheme both introduce an uncertainty of around 1 Tg CH_4/yr .

Table 8. Summary of Modeled Tropospheric Mean CH_4 Burden, CH_4 Sinks due to Tropospheric OH and Cl and CH_4 Chemical Lifetime (τ)

Experiment	CH_4 Burden (Tg)	$\text{CH}_4 + \text{OH}$ Sink (Tg CH_4/yr)	$\text{CH}_4 + \text{Cl}$ Sink (Tg CH_4/yr)	Percent of Total CH_4 Oxidation from Cl	τ_{OH} (Years)	τ_{Cl} (Years)
FULL1	4595	460.2	12.0	2.5	10.0	384.4
FULL1 _{Sim}	4595	460.0	12.9	2.7	10.0	355.6
FULL2	4594	463.0	13.1	2.7	9.9	351.5

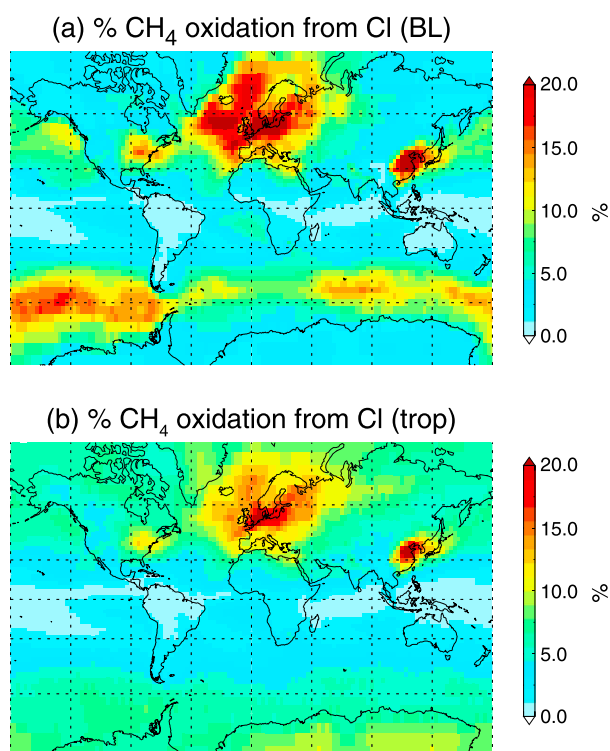


Figure 13. Annual average contribution of Cl atoms to CH₄ oxidation (%) for (a) boundary layer (<1 km) and (b) tropospheric column. Model output from experiment FULL1.

estimated at 430 Gg Cl_y/yr [Sherwen *et al.*, 2016] and is small in comparison to the total Cl_y supplied from the breakdown of CH₃Cl + VSLS (Table 7) and sea-salt dechlorination (section 3.3) considered in our work. On this basis and given that the lower and free troposphere are the regions which make the largest contribution to CH₄ oxidation [Bloss *et al.*, 2005], the exclusion of a tropospheric Cl_y source due to input of stratospheric air is expected to have a relatively small impact on our results. However, the regional and global significance of the above Cl_y sources for tropospheric [Cl] will be investigated in future work (combined, it is anticipated that their inclusion would increase [Cl] and thereby also the CH₄ sink). We also note that the measurement-based estimates of the CH₄ + Cl sink discussed above rely on extrapolation of fairly localized data and therefore carry significant uncertainty. On balance, we suggest that a sink of around 12–13 Tg CH₄/yr from Cl, from this work, constitutes a reasonable conservative estimate, considering that (i) TOMCAT provides a realistic simulation of HCl—the most abundant Cl_y reservoir (section 3.3)—and (ii) that simulated [Cl] is within the expected, albeit large, range from previous evaluations. Overall, the tropospheric loss of CH₄ from Cl is small compared to uncertainty in the tropospheric CH₄ sink from OH, which is >100 Tg CH₄/yr based on bottom-up estimates for 2000–2009 period [Kirschke *et al.*, 2013].

4. Conclusions

We have implemented a detailed representation of tropospheric chlorine chemistry and sources into the TOMCAT global 3-D chemical transport model. The model incorporates the oxidation of chlorocarbons, including various natural and anthropogenic VSLSs, industrial and biomass burning HCl emissions, and a simplified treatment of sea-salt dechlorination. Model simulations were performed to quantify tropospheric [Cl] and to estimate the regional and global importance of Cl atoms as a tropospheric CH₄ sink. We find that tropospheric Cl_y production from chlorocarbons is sensitive to the implementation of chlorocarbon oxidation. When organic chlorine-containing product gases, produced from CH₃Cl, CH₂Cl₂, CHCl₃, C₂Cl₄, CH₂CICH₂Cl, and C₂HCl₃, are considered, total Cl_y production from chlorocarbons (~1400 Gg Cl/yr) is approximately a factor of 3 lower compared to a model run in which all Cl atoms are instantaneously released from

Given uncertainties in both the KIE approach and our process-based modeling, it is difficult to fully reconcile the different estimates discussed above. Notably, there is a large difference (around a factor of 3) between our estimate of 12–13 Tg CH₄/yr and the upper limit of 37 Tg CH₄/yr reported by Platt *et al.* [2004]. Our model estimate may be too conservative given that TOMCAT does not consider all tropospheric Cl_y sources that may be significant. These are potentially numerous and include the persistent degassing of quiescent volcanoes [e.g., Halmer *et al.*, 2002; Aiuppa *et al.*, 2007]; chlorine emissions from terrestrial ecosystems [e.g., Keene *et al.*, 1999]; and relatively localized emissions from, for example, cooling towers and swimming pools [Sarwar and Bhawe, 2007]. As the focus of this work was on Cl_y originating in the troposphere, any influx of Cl_y from the stratosphere [e.g., von Hobe *et al.*, 2011] was also not considered. This source has been

the above gases upon initial oxidation (~ 4320 Gg Cl/yr). Therefore, the assumption of instantaneous Cl_y release from chlorocarbons will likely lead to an overestimate of tropospheric Cl_y production in models. Further work is needed to assess the atmospheric fate of CHClO , which is an organic end product in the oxidation chain of most of the above species and for which no atmospheric observations exist. Based on the chlorine sources considered in our model, we estimate chlorocarbon oxidation accounts for between near zero and 50% of tropospheric Cl_y , depending on altitude.

Compared to the limited observational data, the model provides a realistic simulation of the major chlorine reservoir HCl at numerous sites. In general, boundary layer HCl exceeds several parts per billion at polluted continental sites due to both acid displacement from sea-salt and industrial emissions, though is far lower—typically several hundred parts per trillion—in more remote MBL regions. Simulated tropospheric [Cl] also seems reasonable in comparison to measurement-based estimates, i.e., within the range of 10^3 to 10^5 atoms cm^{-3} [Saiz-Lopez and von Glasow, 2012, and references therein]. Chlorocarbon oxidation provides a small annual mean global [Cl] background of <0.1 to 0.5×10^3 atoms cm^{-3} in the boundary layer, with larger concentrations of up to $\sim 1.0 \times 10^3$ atoms cm^{-3} in some regions during summer months. When both organic and inorganic chlorine sources are considered in the model, simulated surface [Cl] levels exceed 1.0×10^4 atoms cm^{-3} over large areas of the NH. In addition to sea-salt dechlorination, our results show an important role for heterogeneous chlorine reactions on sulfate aerosol which recycle HCl to more reactive forms. With these reactions included, we estimate a tropospheric mean [Cl] (weighted by air mass) of around 1.3×10^3 atoms cm^{-3} .

We estimate a tropospheric CH_4 sink of 12–13 Tg CH_4/yr due to the $\text{CH}_4 + \text{Cl}$ reaction. This is likely a conservative estimate as not all tropospheric chlorine sources were considered and is at the lower limit of previous measurement-derived estimates. In our simulations, Cl atoms account for 2.5 to 2.7% of total tropospheric CH_4 oxidation. This sink is small compared to uncertainty in the global CH_4 sink from OH but nonetheless important to quantify for a thorough understanding of the global methane budget. However, regionally, we calculate that Cl atoms can account for $>20\%$ of boundary layer CH_4 oxidation in some areas. Further constraint on tropospheric [Cl] would be beneficial to help close the atmospheric CH_4 budget and to evaluate the wider role of chlorine in tropospheric chemistry (e.g., as a sink of nonmethane hydrocarbons). Finally, our global model results underpin the notion that active chlorine chemistry is strongly coupled to anthropogenic pollution, as suggested by several regionally focused studies [e.g., Lawler *et al.*, 2009]. On this basis, it seems probable that tropospheric [Cl], and possibly the impact of chlorine chemistry on tropospheric composition, may have changed during the Anthropocene. Given the reactivity of Cl atoms to a wide range of climate-relevant gases, such an area should be examined from a climate forcing perspective in future research.

Acknowledgments

This work was supported by the Natural Environment Research Council (NERC) through the TropHAL project (NE/J02449X/1) and a NERC IRF (NE/N014375/1). R.H. thanks NERC for a research fellowship. M.P.C. thanks the Royal Society for a Wolfson Research Merit Award. The modeling work was performed using the Archer and Leeds ARC2 high-performance computing facilities. The HIPPO data [Wofsy *et al.*, 2016] used in this paper are publicly available at <http://www.eol.ucar.edu/projects/hippo>. Model output is available from Ryan Hossaini.

References

- Aiuppa, A., A. Franco, R. von Glasow, A. G. Allen, W. D' Alessandro, T. A. Mather, D. M. Pyle, and M. Valenza (2007), The tropospheric processing of acidic gases and hydrogen sulphide in volcanic gas plumes as inferred from field and model investigations, *Atmos. Chem. Phys.*, 7(5), 1441–1450, doi:10.5194/acp-7-1441-2007.
- Alexander, B., R. J. Park, D. J. Jacob, Q. B. Li, R. M. Yantosca, J. Savarino, C. C. W. Lee, and M. H. Thieme (2005), Sulfate formation in sea-salt aerosols: Constraints from oxygen isotopes, *J. Geophys. Res.*, 110, D10307, doi:10.1029/2004JD005659.
- Allan, W., H. Struthers, and D. C. Lowe (2007), Methane carbon isotope effects caused by atomic chlorine in the marine boundary layer: Global model results compared with southern hemisphere measurements, *J. Geophys. Res.*, 112, D04306, doi:10.1029/2006JD007369.
- Allegri, I., F. Santis, A. Febo, A. Liberti, and M. Possanzini (1984), Evaluation of atmospheric acidity—Sampling and analytical techniques, in *Physico-Chemical Behaviour of Atmospheric Pollutants*, edited by B. Versino and G. Angeletti, pp. 12–19, Springer, Netherlands, doi:10.1007/978-94-009-6505-8_2.
- Appel, B., Y. Tokiwa, V. Povard, and E. Kothny (1991), The measurement of atmospheric hydrochloric acid in Southern California, *Atmos. Environ. Gen. Top.*, 25(2), 525–527.
- Atkinson, R., D. L. Baulch, R. A. Cox, J. N. Crowley, R. F. Hampson, R. G. Hynes, M. E. Jenkin, M. J. Rossi, and J. Troe (2004), Evaluated kinetic and photochemical data for atmospheric chemistry: Volume I—Gas phase reactions of O_x , HO_x , NO_x and SO_x species, *Atmos. Chem. Phys.*, 4(6), 1461–1738, doi:10.5194/acp-4-1461-2004.
- Atkinson, R., D. L. Baulch, R. A. Cox, J. N. Crowley, R. F. Hampson, R. G. Hynes, M. E. Jenkin, M. J. Rossi, J. Troe, and I. U. P. A. C. Subcommittee (2006), Evaluated kinetic and photochemical data for atmospheric chemistry: Volume II—Gas phase reactions of organic species, *Atmos. Chem. Phys.*, 6(11), 3625–4055, doi:10.5194/acp-6-3625-2006.
- Atkinson, R., D. L. Baulch, R. A. Cox, J. N. Crowley, R. F. Hampson, R. G. Hynes, M. E. Jenkin, M. J. Rossi, and J. Troe (2007), Evaluated kinetic and photochemical data for atmospheric chemistry: Volume III—Gas phase reactions of inorganic halogens, *Atmos. Chem. Phys.*, 7(4), 981–1191, doi:10.5194/acp-7-981-2007.
- Atkinson, R., D. L. Baulch, R. A. Cox, J. N. Crowley, R. F. Hampson, R. G. Hynes, M. E. Jenkin, M. J. Rossi, J. Troe, and T. J. Wallington (2008), Evaluated kinetic and photochemical data for atmospheric chemistry: Volume IV—Gas phase reactions of organic halogen species, *Atmos. Chem. Phys.*, 8(15), 4141–4496, doi:10.5194/acp-8-4141-2008.

- Bannan, T. J., et al. (2015), The first UK measurements of nitryl chloride using a chemical ionization mass spectrometer in central London in the summer of 2012, and an investigation of the role of Cl atom oxidation, *J. Geophys. Res. Atmos.*, *120*, 5638–5657, doi:10.1002/2014JD022629.
- Bari, A., V. Ferraro, L. Wilson, D. Luttinger, and L. Husain (2003), Measurements of gaseous HONO, HNO₃, SO₂, HCl, NH₃, particulate sulfate and PM_{2.5} in New York, NY, *Atmos. Environ.*, *37*(20), 2825–2835, doi:10.1016/S1352-2310(03)00199-7.
- Bartlett, W. P., and D. W. Margerum (1999), Temperature dependencies of the Henry's law constant and the aqueous phase dissociation constant of bromine chloride, *Environ. Sci. Technol.*, *33*(19), 3410–3414, doi:10.1021/es990300k.
- Behnke, W., C. George, V. Scheer, and C. Zetzsch (1997), Production and decay of ClNO₂ from the reaction of gaseous N₂O₅ with NaCl solution: Bulk and aerosol experiments, *J. Geophys. Res.*, *102*(D3), 3795–3804, doi:10.1029/96JD03057.
- Biggs, P., C. E. Canosa-Mas, C. J. Percival, D. E. Shallcross, and R. P. Wayne (1999), A study of the self reaction of CH₂ClO₂ and CHCl₂O₂ radicals at 298 K, *Int. J. Chem. Kinet.*, *31*(6), 433–444, doi:10.1002/(SICI)1097-4601(1999)31:6<433::AID-KIN5>3.0.CO;2-E.
- Bilde, M., J. J. Orlando, G. S. Tyndall, T. J. Wallington, M. D. Hurley, and E. W. Kaiser (1999), FT-IR product studies of the Cl-initiated oxidation of CH₃Cl in the presence of NO, *J. Phys. Chem. A*, *103*(20), 3963–3968, doi:10.1021/jp984523t.
- Bloss, W. J., M. J. Evans, J. D. Lee, R. Sommariva, D. Heard, and M. J. Pilling (2005), Coupling of field measurements of OH and a global chemistry transport model, *Faraday Discuss.*, *130*, 425–436, doi:10.1039/B419090D.
- Breider, T. J. (2010), Coupled halogen-sulfur-aerosol modelling in a 3D chemical transport model, *PhD thesis*, University of Leeds.
- Breider, T. J., M. P. Chipperfield, G. W. Mann, M. T. Woodhouse, and K. S. Carslaw (2015), Suppression of CCN formation by bromine chemistry in the remote marine atmosphere, *Atmos. Sci. Lett.*, *16*(2), 141–147, doi:10.1002/asl2.539.
- Breider, T. J., M. P. Chipperfield, N. A. D. Richards, K. S. Carslaw, G. W. Mann, and D. V. Spracklen (2010), Impact of BrO on dimethyl sulfide in the remote marine boundary layer, *Geophys. Res. Lett.*, *37*, L02807, doi:10.1029/2009GL040868.
- Brimblecombe, P., and S. L. Clegg (1988), The solubility and behaviour of acid gases in the marine aerosol, *J. Atmos. Chem.*, *7*(1), 1–18, doi:10.1007/BF00048251.
- Burkholder, J. B., et al. (2015), Chemical kinetics and photochemical data for use in atmospheric studies, Evaluation number 18, JPL Publication 15-10, Jet Propulsion Laboratory.
- Caloz, F., F. F. Fenter, and M. J. Rossi (1996), Heterogeneous kinetics of the uptake of ClONO₂ on NaCl and KBr, *J. Phys. Chem.*, *100*(18), 7494–7501, doi:10.1021/jp953099i.
- Carpenter, L., et al. (2014), Ozone-depleting substances (ODSs) and other gases of interest to the Montreal Protocol, in: Scientific Assessment of Ozone Depletion: 2014, in *Global Ozone Research and Monitoring Project, Report No. 55* chap. 1, World Meteorol. Organ., Geneva, Switzerland.
- Carpenter, L. J., S. M. MacDonald, M. D. Shaw, R. Kumar, R. W. Saunders, R. Parthipan, J. Wilson, and J. M. C. Plane (2013), Atmospheric iodine levels influenced by sea surface emissions of inorganic iodine, *Nat. Geosci.*, *6*(2), 108–111, doi:10.1038/NGEO1687.
- Catoire, V., R. Lesclaux, W. F. Schneider, and T. J. Wallington (1996), Kinetics and mechanisms of the self-reactions of CCl₃O₂ and CHCl₂O₂ radicals and their reactions with HO₂, *J. Phys. Chem.*, *100*(34), 14,356–14,371, doi:10.1021/jp960572z.
- Catoire, V., P. A. Ariya, H. Niki, and G. W. Harris (1997), FTIR study of the Cl- and Br-atom initiated oxidation of trichloroethylene, *Int. J. Chem. Kinet.*, *29*(9), 695–704, doi:10.1002/(SICI)1097-4601(1997)29:9<695::AID-KIN7>3.0.CO;2-P.
- Chipperfield, M. P. (2006), New version of the TOMCAT/SLIMCAT off-line chemical transport model: Intercomparison of stratospheric tracer experiments, *Q. J. R. Meteorol. Soc.*, *132*(617), 1179–1203, doi:10.1256/qj.05.51.
- Christiansen, C. J., and J. S. Francisco (2010a), Atmospheric Oxidation of Tetrachloroethylene: An Ab Initio Study, *J. Phys. Chem. A*, *114*(34), 9177–9191, doi:10.1021/jp103845h.
- Christiansen, C. J., and J. S. Francisco (2010b), Atmospheric Oxidation of Trichloroethylene: An Ab Initio Study, *J. Phys. Chem. A*, *114*(34), 9163–9176, doi:10.1021/jp103769z.
- Crisp, T. A., B. M. Lerner, E. J. Williams, P. K. Quinn, T. S. Bates, and T. H. Bertram (2014), Observations of gas phase hydrochloric acid in the polluted marine boundary layer, *J. Geophys. Res. Atmos.*, *119*, 6897–6915, doi:10.1002/2013JD020992.
- Dasgupta, P. K., S. W. Campbell, R. S. Al-Horr, S. M. R. Ullah, J. Li, C. Amalfitano, and N. D. Poor (2007), Conversion of sea salt aerosol to NaNO₃ and the production of HCl: Analysis of temporal behaviour of aerosol chloride/nitrate and gaseous HCl/HNO₃ concentrations with AIM, *Atmos. Environ.*, *41*(20), 4242–4257, doi:10.1016/j.atmosenv.2006.09.054.
- de Bruyn, W. J., J. A. Shorter, P. Davidovits, D. R. Worsnop, M. S. Zahniser, and C. E. Kolb (1995), Uptake of haloacetyl and carbonyl halides by water surfaces, *Environ. Sci. Technol.*, *29*(5), 1179–1185, doi:10.1021/es00005a007.
- Dee, D. P., et al. (2011), The ERA-Interim reanalysis: Configuration and performance of the data assimilation system, *Q. J. R. Meteorol. Soc.*, *137*(656), 553–597, doi:10.1002/qj.828.
- Dimmock, N., and G. Marshall (1987), The determination of hydrogen chloride in ambient air with diffusion/denuder tubes, *Anal. Chim. Acta*, *202*, 49–59, doi:10.1016/S0003-2670(00)85901-2.
- Emmons, L. K., et al. (2010), Description and evaluation of the Model for Ozone and Related chemical Tracers, version 4 (MOZART-4), *Geosci. Model Dev.*, *3*(1), 43–67, doi:10.5194/gmd-3-43-2010.
- Emmons, L. K., et al. (2015), The POLARCAT Model Intercomparison Project (POLMIP): Overview and evaluation with observations, *Atmos. Chem. Phys.*, *15*, 6721–6744, doi:10.5194/acp-15-6721-2015.
- Erickson, D. J., C. Seuzaret, W. C. Keene, and S. L. Gong (1999), A general circulation model based calculation of HCl and ClNO₂ production from sea salt dechlorination: Reactive chlorine emissions inventory, *J. Geophys. Res.*, *104*, 8347–8372, doi:10.1029/98JD01384.
- Eriksson, E. (1959), The yearly circulation of chloride and sulfur in nature; meteorological, geochemical and pedological implications. Part 1, *Tellus*, *11*(4), 375–403.
- Erisman, J.-W., A. W. Vermetten, W. A. Asman, A. Waijers-Ijpelaar, and J. Slanina (1988), Vertical distribution of gases and aerosols—The behaviour of ammonia and related components in the lower atmosphere, *Atmos. Environ.*, *22*(6), 1153–1160, doi:10.1016/0004-6981(88)90345-9.
- Evans, M. J., and D. J. Jacob (2005), Impact of new laboratory studies of N₂O₅ hydrolysis on global model budgets of tropospheric nitrogen oxides, ozone, and OH, *Geophys. Res. Lett.*, *32*, L09813, doi:10.1029/2005GL022469.
- Feng, W., M. P. Chipperfield, S. Dhomse, B. M. Monge-Sanz, X. Yang, K. Zhang, and M. Ramonet (2011), Evaluation of cloud convection and tracer transport in a three-dimensional chemical transport model, *Atmos. Chem. Phys.*, *11*(12), 5783–5803, doi:10.5194/acp-11-5783-2011.
- Fernandez, R. P., R. J. Salawitch, D. E. Kinnison, J.-F. Lamarque, and A. Saiz-Lopez (2014), Bromine partitioning in the tropical tropopause layer: Implications for stratospheric injection, *Atmos. Chem. Phys.*, *14*(24), 13,391–13,410, doi:10.5194/acp-14-13391-2014.
- Finlayson-Pitts, B., M. Ezell, and J. Pitts (1989), Formation of chemically active chlorine compounds by reactions of atmospheric NaCl particles with gaseous N₂O₅ and ClONO₂, *Nature*, *337*(6204), 241–244, doi:10.1038/337241a0.
- Finley, B. D., and E. S. Saltzman (2006), Measurement of Cl₂ in coastal urban air, *Geophys. Res. Lett.*, *33*, L11809, doi:10.1029/2006GL025799.

- Finley, B. D., and E. S. Saltzman (2008), Observations of Cl₂, Br₂, and I₂ in coastal marine air, *J. Geophys. Res.*, *113*, D21301, doi:10.1029/2008JD010269.
- Folberth, G. A., D. A. Hauglustaine, J. Lathière, and F. Brocheton (2006), Interactive chemistry in the Laboratoire de Météorologie Dynamique general circulation model: Model description and impact analysis of biogenic hydrocarbons on tropospheric chemistry, *Atmos. Chem. Phys.*, *6*(8), 2273–2319, doi:10.5194/acp-6-2273-2006.
- Gebel, M. E., and B. J. Finlayson-Pitts (2001), Uptake and reaction of ClNO₂ on NaCl and synthetic sea salt, *J. Phys. Chem. A*, *105*(21), 5178–5187, doi:10.1021/jp0046290.
- Giannakopoulos, C., M. Chipperfield, K. Law, and J. Pyle (1999), Validation and intercomparison of wet and dry deposition schemes using Pb-210 in a global three-dimensional off-line chemical transport model, *J. Geophys. Res.*, *104*, 23,761–23,784, doi:10.1029/1999JD900392.
- Gounon, J., and A. Milhau (1986), Incinerator emissions of heavy metals and particulates specialized seminar analysis of inorganic pollutants emitted by the City of Paris garbage incineration plants, *Waste Manage. Res.*, *4*(1), 95–104, doi:10.1177/0734242x8600400111.
- Graedel, T. W., and W. C. Keene (1995), Tropospheric budget of reactive chlorine, *Global Biogeochem. Cycles*, *9*, 47–77, doi:10.1029/94GB03103.
- Granier, C., J. Lamarque, A. Mieville, J. Muller, J. Olivier, J. Orlando, J. Peters, G. Petron, G. Tyndall, and S. Wallens (2005), POET, a database of surface emissions of ozone precursors. [Available at <http://www.aero.jussieu.fr/projet/ACCENT/POET.php>.]
- Grosjean, D. (1990), Liquid-chromatography analysis of chloride and nitrate with negative ultraviolet detection: Ambient levels and relative abundance of gas-phase inorganic and organic acids in Southern California, *Environ. Sci. Technol.*, *24*(1), 77–81, doi:10.1021/es00071a007.
- Guimbaud, C., F. Arens, L. Gutzwiller, H. W. Gaggeler, and M. Ammann (2002), Uptake of HNO₃ to deliquescent sea-salt particles: A study using the short-lived radioactive isotope tracer ¹³N, *Atmos. Chem. Phys.*, *2*(4), 249–257, doi:10.5194/acp-2-249-2002.
- Halmer, M., H.-U. Schmincke, and H.-F. Graf (2002), The annual volcanic gas input into the atmosphere, in particular into the stratosphere: A global data set for the past 100 years, *J. Volcanol. Geotherm. Res.*, *115*(3/4), 511–528, doi:10.1016/S0377-0273(01)00318-3.
- Harrison, R., and A. Allen (1990), Measurements of atmospheric HNO₃, HCl and associated species on a small network in eastern England, *Atmos. Environ. Gen. Top.*, *24*(2), 369–376, doi:10.1016/0960-1686(90)90116-5.
- Holtslag, A., and B. Boville (1993), Local versus nonlocal boundary-layer diffusion in a global climate model, *J. Clim.*, *6*(10), 1825–1842.
- Hossaini, R., et al. (2013), Evaluating global emission inventories of biogenic bromocarbons, *Atmos. Chem. Phys.*, *13*(23), 11,819–11,838, doi:10.5194/acp-13-11819-2013.
- Hossaini, R., M. P. Chipperfield, S. A. Montzka, A. Rap, S. Dhomse, and W. Feng (2015a), Efficiency of short-lived halogens at influencing climate through depletion of stratospheric ozone, *Nat. Geosci.*, *8*, 186–190, doi:10.1038/ngeo2363.
- Hossaini, R., et al. (2015b), Growth in stratospheric chlorine from short-lived chemicals not controlled by the Montreal Protocol, *Geophys. Res. Lett.*, *42*, 4573–4580, doi:10.1002/2015GL063783.
- Hossaini, R., et al. (2016), A multi-model intercomparison of halogenated very short-lived substances (TransCom-VLSL): Linking oceanic emissions and tropospheric transport for a reconciled estimate of the stratospheric source gas injection of bromine, *Atmos. Chem. Phys.*, *16*, 9163–9187, doi:10.5194/acp-16-9163-2016.
- Hough, A. (1988), *The Calculation of Photolysis Rates for Use in Global Tropospheric Modelling Studies*, AERE Report R-13259, HMSO, London.
- Huthwelker, T., T. Peter, B. P. Luo, S. L. Clegg, K. S. Carslaw, and P. Brimblecombe (1995), Solubility of HOCl in water and aqueous H₂SO₄ to stratospheric temperatures, *J. Atmos. Chem.*, *21*(1), 81–95, doi:10.1007/BF00712439.
- Iwasaki, Y., N. Yoshiharu, and N. Tanikawa (1985), High concentration of hydrogen chloride in the atmosphere, Tokyo-to Kogai Kankyusho Nenpo, pp. 3–6, Tokyo Kogai Kankyusho, Tokyo.
- Jacob, D. J. (2000), Heterogeneous chemistry and tropospheric ozone, *Atmos. Environ.*, *34*(12/14), 2131–2159, doi:10.1016/S1352-2310(99)00462-8.
- John, W., S. M. Wall, and J. L. Ondo (1988), A new method for nitric acid and nitrate aerosol measurement using the dichotomous sampler, *Atmos. Environ.*, *22*(8), 1627–1635, doi:10.1016/0004-6981(88)90390-3.
- Johnson, C., L. Sigg, and J. Zobrist (1987), Case studies on the chemical composition of fogwater: The influence of local gaseous emissions, *Atmos. Environ.*, *21*(11), 2365–2374, doi:10.1016/0004-6981(87)90371-4.
- Jourdain, B., and M. Legrand (2002), Year-round records of bulk and size-segregated aerosol composition and HCl and HNO₃ levels in the Dumont D'urville (coastal Antarctica) atmosphere: Implications for sea-salt aerosol fractionation in the winter and summer, *J. Geophys. Res.*, *107*, 4645, doi:10.1029/2002JD002471.
- Kavanaugh, M. C., and R. Trussell (1980), Design of aeration towers to strip volatile contaminants from drinking water, *J. Am. Water Works Assoc.*, *72*(12), 684–692.
- Keene, W. C., and D. L. Savoie (1998), The pH of deliquesced sea-salt aerosol in polluted marine air, *Geophys. Res. Lett.*, *25*, 2181–2184, doi:10.1029/98GL01591.
- Keene, W. C., A. A. P. Pszenny, D. J. Jacob, R. A. Duce, J. N. Galloway, J. J. Schultz-Tokos, H. Sievering, and J. F. Boatman (1990), The geochemical cycling of reactive chlorine through the marine troposphere, *Global Biogeochem. Cycles*, *4*, 407–430, doi:10.1029/GB004i004p00407.
- Keene, W. C., et al. (1999), Composite global emissions of reactive chlorine from anthropogenic and natural sources: Reactive chlorine emissions inventory, *J. Geophys. Res.*, *104*, 8429–8440, doi:10.1029/1998JD100084.
- Keene, W. C., J. Stutz, A. A. P. Pszenny, J. R. Maben, E. V. Fischer, A. M. Smith, R. von Glasow, S. Pechtl, B. C. Sive, and R. K. Varner (2007), Inorganic chlorine and bromine in coastal New England air during summer, *J. Geophys. Res.*, *112*, D10S12, doi:10.1029/2006JD007689.
- Keuken, M., C. Schoonebeek, A. Vanwensenlouter, and J. Slanina (1988), Simultaneous sampling of NH₃, HNO₃, HCl, SO₂ and H₂O₂ in ambient air by a wet annular denuder system, *Atmos. Environ.*, *22*(11), 2541–2548, doi:10.1016/0004-6981(88)90486-6.
- Kim, S., et al. (2008), Airborne measurements of HCl from the marine boundary layer to the lower stratosphere over the North Pacific Ocean during INTEX-B, *Atmos. Chem. Phys. Discuss.*, *8*(1), 3563–3595, doi:10.5194/acpd-8-3563-2008.
- Kindler, T. P., W. L. Chameides, P. H. Wine, D. M. Cunnold, F. N. Alyea, and J. A. Franklin (1995), The fate of atmospheric phosgene and the stratospheric chlorine loadings of its parent compounds: CCl₄, C₂Cl₄, C₂HCl₃, CH₃CCl₃, and CHCl₃, *J. Geophys. Res.*, *100*, 1235–1251, doi:10.1029/94JD02518.
- Kinnison, D. E., et al. (2007), Sensitivity of chemical tracers to meteorological parameters in the MOZART-3 chemical transport model, *J. Geophys. Res.*, *112*, D20302, doi:10.1029/2006JD007879.
- Kirschke, S., et al. (2013), Three decades of global methane sources and sinks, *Nat. Geosci.*, *6*(10), 813–823, doi:10.1038/NNGEO1955.
- Ko, K., et al. (2003), Halogenated very short-lived substances, in: Scientific Assessment of Ozone Depletion: 2006, in *Global Ozone Research and Monitoring Project, Report No. 50* chap. 2, World Meteorological Organization, Geneva, Switzerland.
- Krysztófiak, G., V. Catoire, G. Poulet, V. Maréchal, M. Pirre, F. Louis, S. Canneaux, and B. Josse (2012), Detailed modeling of the atmospheric degradation mechanism of very-short lived brominated species, *Atmos. Environ.*, *59*, 514–532, doi:10.1016/j.atmosenv.2012.05.026.

- Lawler, M. J., B. D. Finley, W. C. Keene, A. A. P. Pszenny, K. A. Read, R. von Glasow, and E. S. Saltzman (2009), Pollution-enhanced reactive chlorine chemistry in the eastern tropical Atlantic boundary layer, *Geophys. Res. Lett.*, *36*, L08810, doi:10.1029/2008GL036666.
- Lawler, M. J., R. Sander, L. J. Carpenter, J. D. Lee, R. von Glasow, R. Sommariva, and E. S. Saltzman (2011), HOCl and Cl₂ observations in marine air, *Atmos. Chem. Phys.*, *11*(15), 7617–7628, doi:10.5194/acp-11-7617-2011.
- Libuda, H. G., F. Zabel, E. H. Fink, and K. H. Becker (1990), Formyl chloride: UV absorption cross sections and rate constants for the reactions with Cl and OH, *J. Phys. Chem.*, *94*(15), 5860–5865, doi:10.1021/j100378a047.
- Lindgren, P. (1992), Diffusion scrubber-ion chromatography for the measurement of trace levels of atmospheric HCl, *Atmos. Environ. Gen. Top.*, *26*(1), 43–49, doi:10.1016/0960-1686(92)90259-N.
- Lober, J. M., W. C. Keene, J. A. Logan, and R. Yevich (1999), Global chlorine emissions from biomass burning: Reactive chlorine emissions inventory, *J. Geophys. Res.*, *104*, 8373–8389, doi:10.1029/1998JD100077.
- Long, M. S., W. C. Keene, R. C. Easter, R. Sander, X. Liu, A. Kerkweg, and D. Erickson (2014), Sensitivity of tropospheric chemical composition to halogen-radical chemistry using a fully coupled size-resolved multiphase chemistry global climate system: Halogen distributions, aerosol composition, and sensitivity of climate-relevant gases, *Atmos. Chem. Phys.*, *14*(7), 3397–3425, doi:10.5194/acp-14-3397-2014.
- Maben, J., W. Keene, A. Pszenny, and J. Galloway (1995), Volatile inorganic Cl in surface air over eastern North America, *Geophys. Res. Lett.*, *22*, 3513–3516, doi:10.1029/95GL03335.
- MacDonald, S. M., J. C. Gómez Martín, R. Chance, S. Warriner, A. Saiz-Lopez, L. J. Carpenter, and J. M. C. Plane (2014), A laboratory characterisation of inorganic iodine emissions from the sea surface: Dependence on oceanic variables and parameterisation for global modelling, *Atmos. Chem. Phys.*, *14*(11), 5841–5852, doi:10.5194/acp-14-5841-2014.
- Mann, G. W., K. S. Carslaw, D. V. Spracklen, D. A. Ridley, P. T. Manktelow, M. P. Chipperfield, S. J. Pickering, and C. E. Johnson (2010), Description and evaluation of GLOMAP-mode: A modal global aerosol microphysics model for the UKCA composition-climate model, *Geosci. Model Dev.*, *3*(2), 519–551, doi:10.5194/gmd-3-519-2010.
- Marché, P., A. Barbe, C. Secroun, J. Corr, and P. Jouve (1980), Ground based spectroscopic measurements of HCl, *Geophys. Res. Lett.*, *7*, 869–872, doi:10.1029/GL0071011p00869.
- Matsumoto, M., and T. Okita (1998), Long term measurements of atmospheric gaseous and aerosol species using an annular denuder system in Nara, Japan, *Atmos. Environ.*, *32*(8), 1419–1425, doi:10.1016/S1352-2310(97)00270-7.
- Matusca, P., B. Schwarz, and K. Bchmann (1984), Measurements of diurnal concentration variations of gaseous HCl in air in the sub-nanogram range, *Atmos. Environ.*, *18*(8), 1667–1675, doi:10.1016/0004-6981(84)90389-5.
- McCulloch, A., M. L. Aucott, C. M. Benkovitz, T. E. Graedel, G. Kleiman, P. M. Midgley, and Y.-F. Li (1999), Global emissions of hydrogen chloride and chloromethane from coal combustion, incineration and industrial activities: Reactive chlorine emissions inventory, *J. Geophys. Res.*, *104*, 8391–8403, doi:10.1029/1999JD900025.
- Mielke, L. H., A. Furgeson, and H. D. Osthoff (2011), Observation of ClNO₂ in a mid-continental urban environment, *Environ. Sci. Technol.*, *45*(20), 8889–8896, doi:10.1021/es201955u.
- Mogili, P. K., P. D. Kleiber, M. A. Young, and V. H. Grassian (2006), N₂O₅ hydrolysis on the components of mineral dust and sea salt aerosol: Comparison study in an environmental aerosol reaction chamber, *Atmos. Environ.*, *40*, 7401–7408, doi:10.1016/j.atmosenv.2006.06.048.
- Molina, M., and F. Rowland (1974), Stratospheric sink for chlorofluoromethane—Chlorine atomic-catalysed destruction of ozone, *Nature*, *249*(5460), 810–812, doi:10.1038/249810a0.
- Monks, S. A., S. R. Arnold, and M. P. Chipperfield (2012), Evidence for El Niño–Southern Oscillation (ENSO) influence on Arctic CO interannual variability through biomass burning emissions, *Geophys. Res. Lett.*, *39*, L14804, doi:10.1029/2012GL052512.
- Monks, S. A., et al. (2016), The TOMCAT global chemical transport model: Description of chemical mechanism and model evaluation, *Geosci. Model Dev. Discuss.*, doi:10.5194/gmd-2016-212.
- Olkhov, R. V., and I. W. M. Smith (2004), Time-resolved experiments on the chlorine atom initiated oxidation of tetrachloroethene, *J. Phys. Chem. A*, *108*(12), 2232–2237, doi:10.1021/jp031158j.
- Ordóñez, C., J.-F. Lamarque, S. Tilmes, D. E. Kinnison, E. L. Atlas, D. R. Blake, G. S. Santos, G. Brasseur, and A. Saiz-Lopez (2012), Bromine and iodine chemistry in a global chemistry-climate model: Description and evaluation of very short-lived oceanic sources, *Atmos. Chem. Phys.*, *12*(3), 1423–1447, doi:10.5194/acp-12-1423-2012.
- Osthoff, H. D., et al. (2008), High levels of nitryl chloride in the polluted subtropical marine boundary layer, *Nat. Geosci.*, *1*(5), 324–328, doi:10.1038/ngeo177.
- Pechtl, S., and R. von Glasow (2007), Reactive chlorine in the marine boundary layer in the outflow of polluted continental air: A model study, *Geophys. Res. Lett.*, *34*, L11813, doi:10.1029/2007GL029761.
- Phillips, G. J., M. J. Tang, J. Thieser, B. Brickwedde, G. Schuster, B. Bohn, J. Lelieveld, and J. N. Crowley (2012), Significant concentrations of nitryl chloride observed in rural continental Europe associated with the influence of sea salt chloride and anthropogenic emissions, *Geophys. Res. Lett.*, *39*, L10811, doi:10.1029/2012GL051912.
- Platt, U., W. Allan, and D. Lowe (2004), Hemispheric average Cl atom concentration from ¹³C/¹²C ratios in atmospheric methane, *Atmos. Chem. Phys.*, *4*, 2393–2399, doi:10.5194/acp-4-2393-2004.
- Pöschl, U., R. von Kuhlmann, N. Poisson, and P. Crutzen (2000), Development and intercomparison of condensed isoprene oxidation mechanisms for global atmospheric modeling, *J. Atmos. Chem.*, *37*(1), 29–52, doi:10.1023/A:1006391009798.
- Prather, M. (1986), Numerical advection by conservation of 2nd-order moments, *J. Geophys. Res.*, *91*, 6671–6681, doi:10.1029/JD091iD06p06671.
- Prather, M. J., C. D. Holmes, and J. Hsu (2012), Reactive greenhouse gas scenarios: Systematic exploration of uncertainties and the role of atmospheric chemistry, *Geophys. Res. Lett.*, *39*, L09803, doi:10.1029/2012GL051440.
- Pszenny, A. A. P., W. C. Keene, D. J. Jacob, S. Fan, J. R. Maben, M. P. Zetwo, M. Springer-Young, and J. N. Galloway (1993), Evidence of inorganic chlorine gases other than hydrogen chloride in marine surface air, *Geophys. Res. Lett.*, *20*, 699–702, doi:10.1029/93GL00047.
- Pszenny, A. A. P., J. Moldanová, W. C. Keene, R. Sander, J. R. Maben, M. Martinez, P. J. Crutzen, D. Perner, and R. G. Prinn (2004), Halogen cycling and aerosol pH in the Hawaiian marine boundary layer, *Atmos. Chem. Phys.*, *4*(1), 147–168, doi:10.5194/acp-4-147-2004.
- Puxbaum, H., E. Quintana, and M. Pimminger (1985), Spatial-distribution of atmospheric aerosol constituents in Linz (Austria), *Fresen. Z. Anal. Chem.*, *322*(2), 205–212, doi:10.1007/BF00517660.
- Rahn, K. A., R. D. Borys, E. L. Butler, and R. A. Duce (1979), Gaseous and particulate halogens in the New York City atmosphere, *Ann. N. Y. Acad. Sci.*, *322*(1), 143–151, doi:10.1111/j.1749-6632.1979.tb14123.x.
- Richards, N. A. D., S. R. Arnold, M. P. Chipperfield, G. Miles, A. Rap, R. Siddans, S. A. Monks, and M. J. Hollaway (2013), The Mediterranean summertime ozone maximum: Global emission sensitivities and radiative impacts, *Atmos. Chem. Phys.*, *13*(5), 2331–2345, doi:10.5194/acp-13-2331-2013.
- Riedel, T. P., et al. (2014), An MCM modelling study of nitryl chloride (ClNO₂) impacts on oxidation, ozone production and nitrogen oxide partitioning in polluted continental outflow, *Atmos. Chem. Phys.*, *14*(8), 3789–3800, doi:10.5194/acp-14-3789-2014.

- Riedel, T. P., et al. (2012), Nitryl chloride and molecular chlorine in the coastal marine boundary layer, *Environ. Sci. Technol.*, *46*(19), 10,463–10,470, doi:10.1021/es204632r.
- Roberts, J. M., H. D. Osthoff, S. S. Brown, A. R. Ravishankara, D. Coffman, P. Quinn, and T. Bates (2009), Laboratory studies of products of N₂O₅ uptake on Cl containing substrates, *Geophys. Res. Lett.*, *36*, L20808, doi:10.1029/2009GL040448.
- Saiz-Lopez, A., and R. von Glasow (2012), Reactive halogen chemistry in the troposphere, *Chem. Soc. Rev.*, *41*, 6448–6472, doi:10.1039/C2CS35208G.
- Saiz-Lopez, A., et al. (2008), On the vertical distribution of boundary layer halogens over coastal Antarctica: Implications for O₃, HO_x, NO_x and the Hg lifetime, *Atmos. Chem. Phys.*, *8*(4), 887–900, doi:10.5194/acp-8-887-2008.
- Saiz-Lopez, A., R. P. Fernandez, C. Ordóñez, D. E. Kinnison, J. C. Gómez Martín, J.-F. Lamarque, and S. Tilmes (2014), Iodine chemistry in the troposphere and its effect on ozone, *Atmos. Chem. Phys.*, *14*(23), 13,119–13,143, doi:10.5194/acp-14-13119-2014.
- Sander, R. (2015), Compilation of Henry's law constants (version 4.0) for water as solvent, *Atmos. Chem. Phys.*, *15*(8), 4399–4981, doi:10.5194/acp-15-4399-2015.
- Sander, R., Y. Rudich, R. von Glasow, and P. J. Crutzen (1999), The role of BrNO₃ in marine tropospheric chemistry: A model study, *Geophys. Res. Lett.*, *26*, 2857–2860, doi:10.1029/1999GL900478.
- Sander, R., et al. (2003), Inorganic bromine in the marine boundary layer: A critical review, *Atmos. Chem. Phys.*, *3*(5), 1301–1336, doi:10.5194/acp-3-1301-2003.
- Sander, R., A. A. P. Pszenny, W. C. Keene, E. Crete, B. Deegan, M. S. Long, J. R. Maben, and A. H. Young (2013), Gas phase acid, ammonia and aerosol ionic and trace element concentrations at Cape Verde during the Reactive Halogens in the Marine Boundary Layer (RHMBLe) 2007 intensive sampling period, *Earth Syst. Sci. Data*, *5*(2), 385–392, doi:10.5194/essd-5-385-2013.
- Sander, S., et al. (2011), Chemical kinetics and photochemical data for use in atmospheric studies, Evaluation number 17, JPL Publication 10-6, Jet Propulsion Laboratory.
- Sanhueza, E., and A. Garaboto (2002), Gaseous HCl at a remote tropical continental site, *Tellus B*, *54*(4), 412–415, doi:10.1034/j.1600-0889.2002.251371.x.
- Sarwar, G., and P. V. Bhawe (2007), Modeling the effect of chlorine emissions on ozone levels over the eastern United States, *J. Appl. Meteorol. Climatol.*, *46*(7), 1009–1019, doi:10.1175/JAM2519.1.
- Sarwar, G., H. Simon, P. Bhawe, and G. Yarwood (2012), Examining the impact of heterogeneous nitryl chloride production on air quality across the United States, *Atmos. Chem. Phys.*, *12*(14), 6455–6473, doi:10.5194/acp-12-6455-2012.
- Schmidt, J. A., et al. (2016), Modeling the tropospheric BrO background: Importance of multiphase chemistry and implications for ozone, OH, and mercury, *J. Geophys. Res. Atmos.*, *121*, 11,819–11,865, doi:10.1002/2015JD024229.
- Sherwen, T., et al. (2016), Global impacts of tropospheric halogens (Cl, Br, I) on oxidants and composition in GEOS-Chem, *Atmos. Chem. Phys.*, *16*, 12,239–12,271, doi:10.5194/acp-16-12239-2016.
- Simmonds, P. G., et al. (2006), Global trends, seasonal cycles, and European emissions of dichloromethane, trichloroethene, and tetrachloroethene from the AGAGE observations at Mace Head, Ireland, and Cape Grim, Tasmania, *J. Geophys. Res.*, *111*, D18304, doi:10.1029/2006JD007082.
- Simpson, W. R., S. S. Brown, A. Saiz-Lopez, J. A. Thornton, and R. von Glasow (2015), Tropospheric halogen chemistry: Sources, cycling, and impacts, *Chem. Rev.*, *115*(10), 4035–4062, doi:10.1021/cr5006638.
- Singh, H. B., and J. F. Kasting (1988), Chlorine-hydrocarbon photochemistry in the marine troposphere and lower stratosphere, *J. Atmos. Chem.*, *7*(3), 261–285, doi:10.1007/BF00130933.
- Sommariva, R., and R. von Glasow (2012), Multiphase halogen chemistry in the tropical Atlantic Ocean, *Environ. Sci. Technol.*, *46*(19), 10,429–10,437, doi:10.1021/es300209f.
- Spicer, C., E. Chapman, B. Finlayson-Pitts, R. Plastringe, J. Hubbe, J. Fast, and C. Berkowitz (1998), Unexpectedly high concentrations of molecular chlorine in coastal air, *Nature*, *394*(6691), 353–356, doi:10.1038/28584.
- Spicer, C. W. (1986), Patterns of atmospheric nitrates, sulfate, and hydrogen chloride in the central Ohio river valley over a one-year period, *Environ. Int.*, *12*(5), 513–518, doi:10.1016/0160-4120(86)90145-5.
- Spracklen, D. V., K. J. Pringle, K. S. Carslaw, M. P. Chipperfield, and G. W. Mann (2005), A global off-line model of size-resolved aerosol microphysics: I. Model development and prediction of aerosol properties, *Atmos. Chem. Phys.*, *5*(8), 2227–2252, doi:10.5194/acp-5-2227-2005.
- Stemmler, K., A. Vlasenko, C. Guimbaud, and M. Ammann (2008), The effect of fatty acid surfactants on the uptake of nitric acid to deliquesced NaCl aerosol, *Atmos. Chem. Phys.*, *8*(17), 5127–5141, doi:10.5194/acp-8-5127-2008.
- Stewart, D. J., P. T. Griffiths, and R. A. Cox (2004), Reactive uptake coefficients for heterogeneous reaction of N₂O₅ with submicron aerosols of NaCl and natural sea salt, *Atmos. Chem. Phys.*, *4*(5), 1381–1388, doi:10.5194/acp-4-1381-2004.
- Stockwell, D., and M. Chipperfield (1999), A tropospheric chemical-transport model: Development and validation of the model transport schemes, *Q. J. R. Meteorol. Soc.*, *125*(557), 1747–1783, doi:10.1256/smsqj.55713.
- Thornton, J. A., et al. (2010), A large atomic chlorine source inferred from mid-continental reactive nitrogen chemistry, *Nature*, *464*(7286), 271–274, doi:10.1038/nature08905.
- Thüner, L. P., I. Barnes, K. H. Becker, T. J. Wallington, L. K. Christensen, J. J. Orlando, and B. Ramacher (1999), Atmospheric chemistry of tetrachloroethene: products of chlorine atom initiated oxidation, *J. Phys. Chem., A*, *103*(43), 8657–8663, doi:10.1021/jp991929c.
- Tiedtke, M. (1989), A comprehensive mass flux scheme for cumulus parameterization in large-scale models, *Mon. Weather Rev.*, *117*(8), 1779–1800, doi:10.1175/1520-0493.
- Timonen, R. S., L. T. Chu, M.-T. Leu, and L. F. Keyser (1994), Heterogeneous reaction of ClNO₂(g) + NaCl(s) → Cl₂(g) + NaNO₂(s), *J. Phys. Chem.*, *98*(38), 9509–9517, doi:10.1021/j100089a025.
- Toyota, K., Y. Kanaya, M. Takahashi, and H. Akimoto (2004), A box model study on photochemical interactions between VOCs and reactive halogen species in the marine boundary layer, *Atmos. Chem. Phys.*, *4*(7), 1961–1987, doi:10.5194/acp-4-1961-2004.
- van der Werf, G. R., J. T. Randerson, L. Giglio, G. J. Collatz, P. S. Kasibhatla, and A. F. Arellano Jr. (2006), Interannual variability in global biomass burning emissions from 1997 to 2004, *Atmos. Chem. Phys.*, *6*(11), 3423–3441, doi:10.5194/acp-6-3423-2006.
- Vogt, R., P. Crutzen, and R. Sander (1996), A mechanism for halogen release from sea-salt aerosol in the remote marine boundary layer, *Nature*, *383*(6598), 327–330, doi:10.1038/383327a0.
- Vogt, R., R. Sander, R. Von Glasow, and P. Crutzen (1999), Iodine chemistry and its role in halogen activation and ozone loss in the marine boundary layer: A model study, *J. Atmos. Chem.*, *32*(3), 375–395, doi:10.1023/A:1006179901037.
- von Glasow, R. (2006), Importance of the surface reaction OH + Cl⁻ on sea salt aerosol for the chemistry of the marine boundary layer—A model study, *Atmos. Chem. Phys.*, *6*(11), 3571–3581, doi:10.5194/acp-6-3571-2006.
- von Glasow, R. (2008), Atmospheric chemistry—Pollution meets sea salt, *Nat. Geosci.*, *1*(5), 292–293, doi:10.1038/ngeo192.

- von Glasow, R., R. Sander, A. Bott, and P. J. Crutzen (2002), Modeling halogen chemistry in the marine boundary layer. 1. Cloud-free MBL, *J. Geophys. Res.*, *107*(D17), 9–16, doi:10.1029/2001JD000942.
- von Hobe, M., et al. (2011), Evidence for heterogeneous chlorine activation in the tropical UTLS, *Atmos. Chem. Phys.*, *11*(1), 241–256, doi:10.5194/acp-11-241-2011.
- Voulgarakis, A., et al. (2013), Analysis of present day and future OH and methane lifetime in the ACCMIP simulations, *Atmos. Chem. Phys.*, *13*(5), 2563–2587, doi:10.5194/acp-13-2563-2013.
- Wagman, P. D., W. H. Evans, V. B. Parker, R. H. Schumm, I. Halow, S. M. Bailey, K. L. Churney, R. L. J. Nuttall (1982), The NBS tables of chemical thermodynamic properties; Selected values for inorganic and C₁ and C₂ organic substances in SI units, *J. Phys. Chem. Ref. Data.*, *11*, suppl. 2.
- Wallington, T. J., M. Bilde, T. E. Møgelberg, J. Sehested, and O. J. Nielsen (1996), Atmospheric Chemistry of 1,2-Dichloroethane: UV Spectra of CH₂ClCHCl and CH₂ClCHClO₂ Radicals, Kinetics of the Reactions of CH₂ClCHCl Radicals with O₂ and CH₂ClCHClO₂ Radicals with NO and NO₂, and Fate of the Alkoxy Radical CH₂ClCHClO, *J. Phys. Chem.*, *100*(14), 5751–5760, doi:10.1021/jp952149g.
- Wild, O., O. V. Rattigan, R. L. Jones, J. A. Pyle, and R. A. Cox (1996), Two-dimensional modelling of some CFC replacement compounds, *J. Atmos. Chem.*, *25*(2), 167–199, doi:10.1007/BF00053790.
- Wingenter, O. W., D. R. Blake, N. J. Blake, B. C. Sive, F. S. Rowland, E. Atlas, and F. Flocke (1999), Tropospheric hydroxyl and atomic chlorine concentrations, and mixing timescales determined from hydrocarbon and halocarbon measurements made over the Southern Ocean, *J. Geophys. Res.*, *104*, 21,819–21,828, doi:10.1029/1999JD900203.
- Wofsy, S. C., et al. (2011), HIPPER Pole-to-Pole Observations (HIPPO): Fine-grained, global-scale measurements of climatically important atmospheric gases and aerosols, *Phil. Trans. R. Soc. A*, *369*(1943), 2073–2086, doi:10.1098/rsta.2010.0313.
- Wofsy, S. C., et al. (2016), *HIPPO Aircraft Data, HIPPO Combined Discrete Flask and GC Sample GHG, Halo-, Hydrocarbon Data (R_20121129)*, Carbon Dioxide Information Analysis Center, Oak Ridge National Laboratory, Oak Ridge, Tenn., doi:10.3334/CDIAC/hippo_012.
- Yang, X., R. Cox, N. Warwick, J. Pyle, G. Carver, F. O' Connor, and N. Savage (2005), Tropospheric bromine chemistry and its impacts on ozone: A model study, *J. Geophys. Res.*, *110*, D23311, doi:10.1029/2005JD006244.
- Yang, X., J. A. Pyle, R. A. Cox, N. Theys, and M. Van Roozendael (2010), Snow-sourced bromine and its implications for polar tropospheric ozone, *Atmos. Chem. Phys.*, *10*(16), 7763–7773, doi:10.5194/acp-10-7763-2010.
- Young, A. H., W. C. Keene, A. A. P. Pszenny, R. Sander, J. A. Thornton, T. P. Riedel, and J. R. Maben (2013), Phase partitioning of soluble trace gases with size-resolved aerosols in near-surface continental air over northern Colorado, USA, during winter, *J. Geophys. Res. Atmos.*, *118*, 9414–9427, doi:10.1002/jgrd.50655.
- Zhang, W., et al. (2009), Asian emissions in 2006 for the NASA INTEX-B mission, *Atmos. Chem. Phys.*, *9*, 5131–5153, doi:10.5194/acp-9-5131-2009.
- Zhou, X., and K. Mopper (1990), Apparent partition coefficients of 15 carbonyl compounds between air and seawater and between air and freshwater; implications for air-sea exchange, *Environ. Sci. Technol.*, *24*(12), 1864–1869, doi:10.1021/es00082a013.
- Ziska, F., et al. (2013), Global sea-to-air flux climatology for bromoform, dibromomethane and methyl iodide, *Atmos. Chem. Phys.*, *13*(2), 8915–8934, doi:10.5194/acpd-13-8915-2013.